Fusarium graminearum DICER-like-dependent sRNAs are required for the suppression of host immune genes and full virulence

Bernhard Werner[1], Aline Koch[2], Ena Šečić[1], Jonas Engelhardt[1], Lukas Jelonek[3], Jens Steinbrenner[1], Karl-Heinz Kogel[1&]

[1]Institute of Phytopathology, Centre for BioSystems, Land Use and Nutrition, Justus Liebig University, Heinrich-Buff-Ring 26-32, D-35392, Giessen, Germany

[2]Institute for Phytomedicine, University of Hohenheim, Otto-Sander-Straße 5, D-70599, Stuttgart, Germany

[3]Institute of Bioinformatics and Systems Biology, Justus Liebig University, Heinrich-Buff-Ring 58, D-35392, Giessen, Germany

Email addresses

Bernhard.T.Werner@online.de

Aline.Koch@uni-hohenheim.de

Ena.Secic@agrar.uni-giessen.de

JonasEngelhardt@yahoo.de

Lukas.Jelonek@computational.bio.uni-giessen.de

Jens.Steinbrenner@agrar.uni-giessen.de

[&]Corresponding author

Karl-Heinz.Kogel@agrar.uni-giessen.de

Abstract

In filamentous fungi, gene silencing by RNA interference (RNAi) shapes many biological processes, including pathogenicity. Recently, fungal small RNAs (sRNAs) have been shown to act as effectors that disrupt gene activity in interacting plant hosts, thereby undermining their defence responses. We show here that the devastating mycotoxin-producing ascomycete *Fusarium graminearum* (*Fg*) utilizes DICER-like (DCL)-dependent sRNAs to target defence genes in two Poaceae hosts, barley (*Hordeum vulgare Hv*) and *Brachypodium distachyon* (*Bd*). We identified 104 *Fg*-sRNAs with sequence homology to host genes that were repressed during interactions of *Fg* and *Hv*, while they accumulated in plants infected by the DCL double knock-out (dKO) mutant PH1-*dcl1/2*. The strength of target gene expression correlated with the abundance of the corresponding *Fg*-sRNA. Specifically, the abundance of three tRNA-derived fragments (tRFs) targeting immunity-related *Ethylene overproducer 1-like 1* (*HvEOL1)* and three Poaceae orthologues of *Arabidopsis thaliana BRI1-associated receptor kinase 1* (*HvBAK1, HvSERK2* and *BdSERK2*) was dependent on fungal DCL. Additionally, RNA-ligase-mediated Rapid Amplification of cDNA Ends (RLM-RACE) identified infection-specific degradation products for the three barley gene transcripts, consistent with the possibility that tRFs contribute to fungal virulence via targeted gene silencing.

Keywords: RNAi, sRNA, *Fusarium graminearum*, DCL, Barley, *Hordeum vulgare*, *Brachypodium distachyon*, SERK, EOL1, BAK1

Significance Statement

Fusarium graminearum is one of the most devastating fungal pathogens in cereals, while understanding the mechanisms of fungal pathogenesis is a prerequisite for developing efficient and environmentally friendly crop protection strategies. We show exploratory data suggesting that fungal small RNAs play a critical role in Fusarium virulence by suppressing plant immunity.

Introduction

RNA interference (RNAi) is a biological process in which small RNA (sRNA) molecules mediate gene silencing at the transcriptional or post-transcriptional level. In agriculture, RNAi-mediated silencing strategies have the potential to protect crops from pests and microbial pathogens (Koch & Kogel 2014; Guo et al. 2016; Liu et al. 2020; Šečić & Kogel 2021; Koch & Wassenegger 2021). Expression of non-coding double-stranded (ds) RNA targeting essential genes in a pest, a pathogen or a virus can render host plants more resistant by a process known as host-induced gene silencing (HIGS) (Rosa et al. 2018; Cai et al. 2018a; Gaffar & Koch 2019; Niehl & Heinlein 2019). Alternatively, plants can be protected by foliar application of dsRNA to plants (Koch et al. 2016; Wang et al. 2016a; Konakalla et al. 2016; Mitter et al. 2017; Kaldis et al. 2018; McLoughin et al. 2018; Sang et al. 2020). While these RNAi-based crop protection strategies are proving to be efficient and agronomically practical in the control of insects (Head et al. 2017) and viruses (Niehl et al. 2018), many questions remain unanswered with regard to the control of fungi.

The blueprint for using RNA to fight disease comes from nature (Cai et al. 2018a). During infection of *Arabidopsis thaliana* (*At*), the necrotrophic ascomycete *Botrytis cinerea* (*Bc*) secretes DICER-like (DCL)-dependent sRNAs that are taken up into plant cells to interact with the Arabidopsis ARGONAUTE protein *At*AGO1 and initiate silencing of plant immune genes (Weiberg et al. 2013; Cai et al. 2018b). For instance, sRNA *Bc*-siR3.2 targets mitogen-activated protein kinases, including *MPK2* and *MPK1* in *At*, and *MAPKKK4* in tomato (*Solanum lycopersicum*), while *Bc*-siR37 targets several immune-related transcription factors including *WRKY7*, *PMR6* and *FEI2* (Wang et al. 2017b). Likewise, the oomycete *Hyaloperonospora arabidopsidis* produces 133 AGO1-bound sRNAs, which are crucial for virulence (Dunker et al. 2020), and microRNA-like RNA1 (*Pst*-milR1) from the yellow rust causing biotrophic basidiomycete *Puccinia striiformis* f.sp. *tritici* (*Pst*) reduced expression of the defence gene

Pathogenesis-related 2 (*PR2*) in wheat (*Triticum aestivum*) (Wang et al 2017a). Notably, when comparing sRNA in the leaf rust fungus *Puccinia triticina* (*Pt*), 38 *Pt*-sRNAs were homologous to sRNAs previously identified in *Pst* (Dubey et al. 2019; Mueth et al. 2015), hinting to the possibility that sRNA effectors are conserved among related fungal species as it is known for plant miRNAs (Reinhart et al. 2002, Jones-Rhoades 2012). One group of conserved sRNAs with putative effector function are transfer RNA (tRNA)-derived fragments (tRFs). Bacterial tRFs play a role in the symbiotic interaction between soybean (*Glycine max*) and its nitrogen fixing symbiont *Bradyrhizobium japonicum* during root nodulation (Ren et al. 2019). Similarly, the protozoan pathogen *Trypanosoma cruzi* secretes tRF-containing microvesicles resulting in gene expression changes in mammalian host cells (Garcia-Silva et al. 2014).

Fungal species of the genus *Fusarium* belong to the most devastating pathogens of cereals causing Fusarium head blight and crown rot (Dean et al., 2012), and contaminate the grain with mycotoxins such as the B group trichothecenes deoxynivalenol (DON), nivalenol (NIV), and their acetylated derivatives (3A-DON, 15A-DON, and 4A-NIV) (Desjardins et al., 1993; Jansen et al., 2005; Ilgen et al., 2009). Viability, aggressiveness, and virulence of Fusaria are under control of the RNAi machinery (Kim et al., 2015; Son et al., 2017; Gaffar et al. 2019).

To test the possibility of *Fg* producing sRNAs that exert effector function and promote pathogenesis, we predicted Fg-sRNA targets in two Poaceae hosts, *Hordeum vulgare* (*Hv*) and *Brachypodium distachyon* (*Bd*). Among the many predicted plant targets of fungal sRNA, three fungal tRFs had sequence similarity to *BRI1-associated receptor kinase 1* (*BAK1*) homologs and *EOL1* (*Ethylene overproducer 1-like 1*) in *Hv* and *Bd*. Upon infection with the wild type *Fg* strain, transcripts of genes were strongly reduced, while in contrast they were increased upon infection with *Fg* strains compromised for DCL activity. Degradation products of target mRNAs were detected by RNA-ligase-mediated Rapid Amplification of cDNA Ends (RLM-

100 RACE), supporting the possibility that DCL-dependent sRNAs play a critical role in the
101 interaction of *Fg* with cereal hosts.

102

Results

Fusarium graminearum DCL mutants are less virulent on barley and Brachypodium leaves

The Fusarium mutant IFA65-*dcl1* is partially impaired in infecting wheat ears and causing Fusarium head blight (Gaffar et al. 2019). We extended this earlier study to examine the effects of impaired DCL activity on the plant defence response. To this end, two to three-week-old detached second leaves of barley cv. Golden Promise (GP) were drop-inoculated with 3 µl of a solution containing 150,000 conidia per ml of *Fg* isolate PH1 or the double knock-out (dKO) mutant PH1-*dcl1/2*. At five days post inoculation (dpi), the dKO mutant produced significantly smaller necrotic lesions (30%; median (MED) (27%); interquartile range (IQR) (47%) Wilcoxon rank sum test, p=0.007) than the wild type (wt) strain, confirming that DCL activity is required for full *Fg* virulence (Fig. 1A).

Next, we determined the virulence of *DCL* mutants on *Brachypodium distachyon* Bd21-3. Flag leaves of three-week-old plants were inoculated with 10 µl (10,000 conidia ml^{-1}) of fungal inoculum. Single mutants IFA65-*dcl1* and IFA65-*dcl2* produced significantly smaller lesions than the wt (IFA65-*dcl1*, 54%; MED (42%); IQR (56%) and IFA65-*dcl2*, 66%; MED (60%); IQR (58%); pairwise Wilcoxon rank sum test; Bonferroni corrected; $p<0.005$) (Fig. 1B). These results substantiate the earlier findings (Gaffar et al. 2019) that fungal DCL activity is required for Fusarium virulence on graminaceous plants.

Selection of sRNAs with sequence homology to plant genes

We looked for interaction-related fungal sRNAs that potentially could interfere with plant gene expression by sequence-specific silencing. To this end, a previously published sRNA sequencing data set of *Fg* sRNAs from an axenic IFA65 culture (Koch et al. 2016) was analysed for sRNAs with sequence complementarity to barley genes. In order to identify a wide range of potential targets, we applied only two selection criteria, namely *i.* size (21-24 nt) and *ii.* a

minimal number of reads (at least 400 reads in the dataset). From a total of 35,997,924 raw reads, 5,462,596 (comprising 589,943 unique sequences) had a length of 21-24 nt. From the unique sequences, 1,987 had at least 400 reads. Since the IFA65 genome has not been sequenced, we used the published genome information of *Fg* strain PH1 (genome assembly ASM24013v3 from International Gibberella zeae Genomics Consortium: GCA_000240135.3) for further analysis. The majority of the 1,987 unique sRNAs mapped to rRNA (64.4%) and intergenic regions (21.6%), while 3.7% and 2.4% mapped to protein coding genes and tRNAs, respectively, and 7.8% did not perfectly match the reference genome (Fig. S1). According to the TAPIR algorithm, the 1,987 sequences overall matched mRNAs of 2,492 genes (Hordeum vulgare IBSC PGSB v2 reference genome; Mascher et al., 2017) sufficiently close according to the refined target prediction criteria suggested by Srivastava et al. (2014). GO-enrichment analysis revealed an enrichment in functions of nucleotide binding, motor activity and kinase activity and processes such as transport and localization (Fig. S2). Most of the 14,156 transcripts of the 2,492 target genes, which we nominated as potential sRNA targets, showed partially homologous sequences to more than one sRNA accounting for a total of 17,275 unique pairs of potential target gene - sRNA combinations. Target prediction results are presented with only one transcript (splice variant) for every combination (Tab. S2). Of note, merely 101 out of the 1,987 sRNAs had no predicted target among the total number of 248,391 plant mRNAs in the IBSC_PGSB_v2 annotation.

Barley immune genes accumulate to higher levels in PH1-dcl1/2-infected leaves

From the set of 2,492 barley genes with partial sequence homology to *Fg* sRNAs, we selected 16 genes for further analysis, based on an educated guess that they are potentially involved in biotic stress reactions during plant-fungal interaction (Tab. 1). When tested with RT-qPCR, we found eight genes significantly higher expressed (Student's *t*-test, paired, *p<0.1, **p<0.05,

152 ***p<0.01) in leaves infected with PH1-*dcl1/2* vs. PH1 (Fig. 2). Among these genes are three
153 that encode proteins involved in the regulation of either ethylene (ET) (Ethylene overproducer
154 1-like 1, *Hv*EOL1) or auxin responses (Auxin response transcription factors *Hv*ARF10 and
155 *Hv*ARF19) and three kinases, of which Somatic embryogenesis receptor-like kinase 2
156 (*Hv*SERK2) and BRI1-associated receptor kinase 1 (*Hv*BAK1) are likely involved in
157 recognition of microbe-associated molecular patterns (MAMPs). Moreover, genes encoding the
158 plastid kinase 2-Phosphoglycolate phosphatase 2 (*Hv*PGLP2), Resurrection 1 (*Hv*RST1, with a
159 rather elusive function in cuticle formation and embryo development), and the histone-lysine
160 N-methyltransferase Su(var)3-9-related protein 5 (*Hv*SUVR5, involved in transcriptional gene
161 silencing) were also strongly expressed.

162 ***HvEOL1 transcripts also accumulate to higher levels upon DCL knock-down via spray***
163 ***induced gene silencing (SIGS)***

164 We selected *HvEOL1* (*HORVU2Hr1G119180*), which is a homologue of *At Ethylene*
165 *overproducer1* (*AtETO1*; *AT4GO2680.1*), for further analysis. The alignment of the respective
166 protein sequences of *Hv*EOL1 and *At*ETO1 is shown in Fig. S3. *At*ETO1 negatively regulates
167 ethylene synthesis in *At* by ubiquitination of type-2 1-Aminocyclopropane-1-carboxylate
168 synthases (ACSs), which produce the direct precursor of ET (Christians et al. 2009) (Fig. S4).
169 Upon inoculation with PH1, *HvEOL1* expression was reduced by 23% as compared to non-
170 inoculated barley leaves. In contrast, *HvEOL1* was strongly expressed in PH1-*dcl1/2*-infected
171 leaves well above the levels measured either in PH1- or mock-inoculated leaves. To further
172 substantiate that *HvEOL1* expression is under the control of fungal DCL activity, we used a
173 SIGS strategy (Koch et al. 2016) to partially inactivate DCL function in *Fg*. Two-week-old
174 detached leaves were sprayed with 20 ng μl^{-1} of dsRNA-*dcl1/2*, a 1,782 nt long dsRNA derived
175 from the sequences of IFA65-*DCL1* and IFA65-*DCL2* (Fig. S5A,B). 48 h later, leaves were
176 drop inoculated with conidia and harvested at 5 dpi. Consistent with the expectation that

177 exogenous dsRNA-*dcl1/2* mediates silencing of their *DCL* gene targets, RT-qPCR analysis
178 confirmed that the transcript levels of IFA65-*DCL1* and IFA65-*DCL2* were reduced to 22%
179 and 42%, respectively, as compared with the Tris-EDTA (TE) buffer control (Fig. 3A). In
180 accordance with the results obtained with strain PH1, *HvEOL1* was also significantly (p=0.029,
181 Student's *t*-test (Δct), one sided, paired) downregulated in response to IFA65 infection
182 compared to mock controls treated with 0.02% Tween20 (Fig. 3B). In contrast, however, when
183 leaves were sprayed with dsRNA-*dcl1/2* prior to inoculation with IFA65, *HvEOL1* transcripts
184 strongly accumulated in comparison with the inoculated leaves sprayed with TE buffer (Fig.
185 3C).

186

187 ***Fungal sRNAs targeting HvBAK1, HvEOL1, and HvSERK2 mRNAs are less abundant in***
188 ***PH1-dcl1/2 vs. PH1***

189 To detect the abundance of specific *Fg*-sRNAs, originally identified by sequencing of axenic
190 IFA65 mycelium, in PH1-infected plant tissue, we performed reverse transcription stem-loop
191 qPCR (Chen et al. 2005). From the above defined pool of 1,987 *Fg*-sRNAs (axenic, 21-24 nt
192 length, >=400 reads) 22 unique sRNAs matched partial sequences of *HvEOL1*, 10 matched
193 *HvBAK1* and five matched *HvSERK2*. *Fg*-sRNA-1921 matched all three genes and *Fg*-sRNA-
194 321 matched both *HvEOL1* and *HvBAK1* (Tab. 2; Tab. S2). These two sRNAs show high
195 sequence similarities among each other. To identify their origin, they were aligned to the
196 genomic sequence of strain PH1 (GCA_900044135.1). We found that they match the gene
197 *Fg_CS3005_tRNA-Gly-GCC-1-9* encoding tRNA-Gly for the anticodon GCC. Of note, a larger
198 cluster of 27 overlapping tRNA-derived fragments (tRFs) with more than 50 reads matching
199 the tRNA-Gly gene sequence were detected (Fig. S6). To assess differential accumulation of
200 tRFs from the *Fg_CS3005_tRNA-Gly-GCC-1-9* cluster in leaves infected with PH1 *vs.* PH1-
201 *dcl1/2*, sRNAs were reverse transcribed using hairpin-priming followed by qPCR amplification

(Chen et al. 2005). For this analysis, we chose *Fg*-sRNA-321, the most abundant tRF from this cluster, along with *Fg*-sRNA-1921, which targets all three GOIs and an additional tRF (*Fg*-sRNA-6717), which targets *HvEOL1* and *HvBAK1* (see Tab. 2) to assess the sensitivity of the assay. In the initial IFA65 dataset the *Fg*-sRNA-321 had a read count of 2,106, *Fg*-sRNA-1921 had 416 and *Fg*-sRNA-6717 had 86 from a total of more than 5 million reads (Fig. S7). This equals 386 reads per million (rpm) for *Fg*-sRNA-321, while in average unique reads had only 1.7 rpm. Using TAPIR (Bonnet et al. 2010), we also calculated the target score values for all three tRFs, which is a measure for the similarity between sRNA and target. A high value refers to more dissimilarities. Mismatches (MMs) increase the score by one point and G-U pairs by 0.5 points. These values are doubled if the respective MMs and G-U pairs are located between the second and 12th nt of the sRNA (5'-3') because a high similarity in the seed region of the sRNA is especially important for RNAi (Mallory et al. 2004). *Fg*-sRNA-321 has a score of 4.5 for *HvBAK1* and *HvEOL1*, *Fg*-sRNA-1921 has a score of 4, 3.5 and 6 for *HvBAK1*, *HvEOL1* and *HvSERK2*, respectively and *Fg*-sRNA-6717 has a score of 5.5 and 4.5 with *HvBAK1* and *HvEOL1*. In plants other than Arabidopsis, such as wheat and rice, a score cut off at 4 or 6 points lead to a precision of 82% or 62% and a recall of known interactions of 39% or 58% respectively according to Srivastava et al. (2014).

All three fungal tRFs were detected in infected leaves, while they could not be found in uninfected leaves (Fig. 4). Significantly lower amounts of *Fg*-sRNA-1921 (59%), *Fg*-sRNA-321 (56%), and *Fg*-sRNA-6717 (60%) were detected in PH1-*dcl1/2 vs*. PH1-infected leaves (Fig. 4), showing that their biogenesis is DCL-dependent.

Fg-sRNA-321 and Fg-sRNA-1921 also match SERK2 in Brachypodium distachyon Bd21-3

Next, we assessed the possibility that *Fg*-sRNA-321, *Fg*-sRNA-1921 and *Fg*-sRNA-6717 also have sequence homologies in *At* and the model grass *Bd*. Target prediction with the TAPIR

227 algorithm using the optimised parameters for *At* (score=4; mfe=0.7), could not detect potential
228 targets in *At* ecotype Col-0. In contrast, these three tRFs matched the sequence of *Brachypodium*
229 *somatic embryogenesis receptor-like kinase 2* (*BdSERK2*) in Bd21-3 with a score of 3.5, 3 and
230 5.5, respectively (Tab. 2). We examined the expression pattern of *BdSERK2* in response to leaf
231 infection: *BdSERK2* is relatively weakly expressed in uninfected plants and is not further
232 suppressed after inoculation with PH1, whereas it strongly accumulated in PH1-*dcl1/2 vs.* PH1-
233 infected Bd21-3 (Fig. 5). This finding further supports the possibility that the control of *SERK2*
234 expression via RNAi pathways by *Fg* is evolutionary conserved in cereals.

235 ***RLM-RACE shows infection specific degradation products of HvBAK1, HvEOL1 and***
236 ***HvSERK2***

237 We assessed the sRNA-mediated cleavage of *HvBAK1*, *HvEOL1*, and *HvSERK2* mRNAs, using
238 a modified RNA-ligase-mediated Rapid Amplification of cDNA Ends (RLM-RACE) assay.
239 Control samples were prepared both from uninfected tissue and from infected tissue without
240 the reverse transcription step (no-RT control) and PCR products were visualized on an EtBr-
241 Agarose gel. In these no-RT controls no amplification was visible.

242 For each gene more than one infection-specific product was amplified (blue and red arrows),
243 which could not be amplified from the uninfected sample (Fig. 6D-F). We excised three bands
244 (red arrows) of the expected size for a *Fg*-sRNA-1921 guided cleavage of *HvBAK1* (Fig. 6D)
245 and one band for *HvEOL1* (Fig. 6E) and *HvSERK2* (Fig. 6F) and cloned them into the pGEM-
246 T easy vector system. According to the IBSC_PGSB_v2 assembly, *HvBAK1* has splice variants,
247 which could produce cleavage products of different lengths while for *HvSERK2* and *HvEOL1*
248 there are no introns between sRNA target site and primer. From each band, five colonies were
249 picked and for 23 of these extracted plasmids sequences were obtained. 16 sequences perfectly
250 matched the reference genome, four with one MM and one with four MMs. Two sequences did
251 not match the reference sufficiently enough to be aligned over the full length. The observed

252 cleavage products are close to but do not match the canonical slice site between the 10th and
253 11th nt of *Fg*-sRNA-1921 and *Fg*-sRNA-321 (Fig. 6A-C).

254

255 ***Total sRNAs predicted to target a gene in barley are correlated with the de-repression***
256 ***strength***

257 Not all potential targets of *Fg*-sRNAs are downregulated nor do all potential targets show a re-
258 accumulation upon infection with PH1-*dcl1/2* (see Fig. 3). To address this bias we conducted a
259 more focused target prediction exclusively for the 16 genes already tested by RT-qPCR. This
260 allowed a much more thorough search, where targets for all sRNAs with at least two reads were
261 predicted. From these 136,825 unique sRNAs (axenic, 21-24 nt length, >=2 reads) representing
262 4,997,312 reads of the total of 5,439,472 reads 21-24 nt in length, 5,052 have potential target
263 sequences in the 16 mRNA sequences selected for further investigation in the *Hordeum vulgare*
264 cv. GP assembly GCA_902500625. An additional filter step was employed to select for sRNAs
265 with a maximum of one MM to the PH1 assemblies GCA_000240135.3 and
266 GCA_900044135.1. Subsequently, sRNAs with up to one MM to *Fg*-rRNAs were removed
267 leaving a total of 1,212 sRNAs with 1,311 potential sRNA-mRNA interactions representing
268 85,531 reads in the analysis.

269 To establish a correlation of the observed resurgence of potential target genes and targeting
270 sRNAs, we analysed the *DCL*-dependent expression change using ΔΔΔct values. To compare
271 the expression of a GOI in two samples, the difference between the ct-values for a reference
272 gene and the GOI can be determined (Δct) and to calculate the expression difference between
273 the control and treated sample the difference between the Δct values (ΔΔct) is calculated. We
274 further defined the ΔΔΔct value as the difference between the ΔΔct values for a GOI in PH1
275 and PH1-*dcl1/2*-infected samples. From this follows a gene with a negative ΔΔΔct value shows
276 a higher transcript accumulation during the infection with a fungal strain with compromised

277 DCL function and the stronger the accumulation the lower this ΔΔΔct value is. We found a
278 negative correlation between the ΔΔΔct value and the number of total sRNAs targeting a GOI
279 (Fig. 7). This correlation becomes more significant if a lower score cut-off for the target
280 prediction is chosen until the cut-off of four. The most significant correlation is for all predicted
281 interactions with a score equal or below four with a p-value of 0.011 (t-test) (Fig. 7B). The p-
282 value for a correlation with a cut-off of five (Fig. 7C) is 0.033 (t-test) and six (Fig. 7D) is 0.094
283 (t-test), while a score cut-off of 3 leads to a situation, where there are no predicted sRNA
284 interactions for all genes except for three (Fig. 7A).

285

286

Discussion

We show here that full virulence of the ascomycete fungus *Fusarium graminearum* on graminaceous leaves depends on the activity of fungal DCLs. The dKO mutant PH1-*dcl1/2* is less virulent on barley and the two single KO mutants IFA65-*dcl1* and IFA65-*dcl2* also are less virulent on *Brachypodium*. These results are consistent with our previous studies showing that knock-down or SIGS-mediated silencing of Fusarium *DCLs* and other components of the RNAi machinery reduced the virulence of the fungus on barley (Gaffar et al. 2019; Werner et al. 2020). DCL enzymes are key components of the fungal RNAi machinery required for the biogenesis of sRNAs directing silencing of sequence-complementary endogenous and foreign genes (Lax et al. 2020). The latter case involves DCL-dependent pathogen-derived sRNAs that target plant defense genes to increase virulence as shown for *Botrytis cinerea* (Weiberg et al. 2013; Wang et al. 2017b), *Puccinia striiformis* (Wang et al.2017a) and *Magnaporthe oryzae* (Zanini et al. 2021).

In the present work we found potential host target genes for fungal small RNAs (*Fg*-sRNAs) that were differentially regulated in response to plant infection with *Fg* wt *vs*. *Fg* DCL KO mutants, and the same effect was confirmed when DCLs were silenced by SIGS. This suggests a scenario in which impaired DCL function resulting in reduced fungal RNAi activity ultimately leads to de-repression of host target genes. Of note, target gene de-repression was also observed when the transcript was not significantly downregulated by the wt fungus during infection. This could be explained by a mutually neutralizing effect in which *Fg*-sRNAs continuously target genes for silencing, while concurrent plant immune responses are a trigger for up-regulation. Thus, one can speculate that these described effects reflect an abrogation of host-favouring upregulation by host immunity *vs*. pathogen-favouring downregulation by sRNA effectors.

We identified three tRFs predicted to target *BdSERK2*, *HvBAK1*, *HvEOL1* and *HvSERK2*. Unexpectedly, these tRFs are partially DCL-dependent, with a reduced abundance by more than

312 50% during infections with the dKO mutant PH1-*dcl1/2 vs.* wt PH1 based on fungal biomass.
313 Current knowledge of tRFs in fungi and oomycetes suggests that their silencing activity is
314 independent of DCL, as shown for *Sclerotinia sclerotiorum* (Lee Marzano et al. 2019) and
315 *Phytophthora infestans*, where the production is partially dependent on AGO (Åsman et al.
316 2014). Furthermore, analysis of tRFs in Cryptococcus spp. revealed a RNAi-independent
317 generation of tRFs and possible compensatory effects in an RNAi-deficient genotype (Streit et
318 al. 2021). Interestingly however, the tRFs *Fg*-sRNA-321, *Fg*-sRNA-1921 and *Fg*-sRNA-6717
319 are neither 5'- or 3' tRNA halves nor do they belong to any of the described tRF-1, tRF-2, tRF-4
320 or tRF-5 classes (Kumar et al. 2016a) applied by the tRFtarget database for animals, yeast
321 (*Schizosaccharomyces pombe*) and the bacterium *Rhodobacter sphaeroides* (Li et al. 2021).
322 When following the classification of the tsRBase used for all eukaryotic kingdoms and bacteria
323 (Zuo et al. 2021), the three tRFs are classified as internal tRFs based on the origin within the
324 mature tRNA. Interestingly, there are tRFs found in *Phytophthora sojae* starting in the
325 anticodon loop and ending in the T loop of mature tRNAs (Wang et al. 2016b), which resembles
326 the Fg-sRNA tRFs (Fig. S8).

327 We observed several infection-specific degradation products of the predicted host target genes
328 *HvBAK1*, *HvEOL1* and *HvSERK2* for tRFs *Fg*-sRNA-321, *Fg*-sRNA-1921 and *Fg*-sRNA-
329 6717. However, cleavage occurred outside the canonical miRNA cleavage site as defined by
330 Mallory et al. (2004), though these genes are partially silenced during infection and silencing
331 is apparently abolished upon infection with the DCL dKO mutant. While the canonical cleavage
332 site for miRNA-directed cleavage in *At* is well defined, the tRF-directed cleavage observed by
333 5' RACE of transposable elements in *At* (Martinez et al. 2017) and of defence-related genes
334 during the infection of black pepper (*Piper nigrum*) with *Phytophthora capsici* (Asha & Soniya
335 2016) was found outside of the canonical cleavage site. Additionally, the identification of
336 sRNA-directed cleavage sites in barley often leads to divergent findings. Ferdous et al. (2017)
337 predicted ~400 target genes for 11 presumably drought responsive miRNAs and found cleavage

products for 15 targets overlapping the respective miRNAs alignment through degradome sequencing in the two barley cultivars Golden Promise (GP) and Pallas. From these confirmed targets, 13 were cleaved at the canonical 10^{th}-11^{th} nt site, one was cleaved at 19^{th}-20^{th} nt, and one at the 5^{th}-6^{th} nt. Hackenberg et al. (2015) predicted 97 target genes of drought responsive miRNAs in GP and identified eight targets through degradome sequencing, which were all cleaved outside of the 10^{th}-11^{th} nt site. Thus, both studies suggest the presence of non-canonical miRNA directed cleavage. Of note, both studies relied on the same degradome sequencing dataset from GP, while Ferdous et al. also observed non-canonical cleavage in an independent Pallas dataset. Moreover, in a study performed by Curaba et al. (2012) 96 target genes of GP for miRNAs involved in seed development and germination were identified by degradome sequencing and only 16 targets were cleaved exclusively at the 10^{th}-11^{th} nt site, while the other targets were sporadically cleaved with an offset (24) and 56 were cleaved in majority in a non-canonical site. Finally, Deng et al. (2015) identify in the barley cultivar Morex 65 target genes of 39 miRNAs, and for only 32% of the identified targets the canonical 10^{th}-11^{th} nt cleavage product was the major degradome product. Together these studies highlight the challenges in the identification of cleavage sites of sRNAs in barley and cleavage sites of tRFs in plants. The absence of canonical cleavage products for tRFs does therefore not exclude the tRF-directed cleavage of *HvBAK1*, *HvEOL1* and *HvSERK2*.

We found that 22 *Fg*-sRNAs target *HvEOL1*, a putative negative regulator of ET biosynthesis in barley. In *Arabidopsis thaliana* the EOL1 homolog *At*ETO1 acts together with *At*EOL1 and *At*ETO1-like 2 (EOL2) in directing the ubiquitination and subsequent degradation of type-2 1-aminocyclopropane-1-carboxylate synthase (ACS) proteins (e.g. ET overproducer 2 (ETO2)) (Christians et al. 2009; Yoshida et al. 2006). ET is a gaseous plant hormone that plays an important role in regulating plant growth and development, and is critical for pathogen interaction and abiotic stresses (Abeles et al. 1992). Generally, ET acts synergistically with jasmonate (JA) in the defence response against necrotrophic pathogens and this ET/JA response

has antagonistic effects on salicylic acid (SA) signalling against biotrophic pathogens. Yet in low amounts JA and SA act synergistically (Glazebrook 2005; Li et al. 2019). Therefore, controlling both ET biosynthesis and ET signalling is crucial for plants. Towards this, plants have evolved complex mechanisms that allow tight regulation of ET pathways e.g. at the level of (i) ET production mainly by regulating ACS gene family members, (ii) ET perception through constitutive triple response 1 (CTR1)-mediated inhibition of positive regulator ET insensitive 2 (EIN2) (Kieber et al. 1993, Alonso et al. 1999), and (iii) expression of ET-responsive TFs (e.g. ET response factor 1 (ERF1)) via EBF-mediated degradation of ET insensitive 3 (EIN3) (Potuschak et al. 2003) (Fig. S4). According to the anticipated role of ET in the plant response to necrotrophic pathogens, such as *Fg*, targeting negative regulators of ET synthesis such as *HvEOL1* would be detrimental to *Fg* colonization. Of note, our findings are consistent with previous results demonstrating that *Fg* exploits ET signalling to enhance colonization of Arabidopsis, wheat and barley (Chen et al. 2009), supposedly through an increase in DON-induced cell death through ET. These findings further challenge the role of ET in defence against necrotrophic pathogens. Strikingly, the authors showed that in Arabidopsis ET overproducing mutants (ETO1 and ETO2) and a negative regulator of ET signalling (CTR1) are more susceptible to *Fg*, while *At* mutants in ET perception (ETR1) and signalling (EIN2 and EIN3) are resistant. These findings were confirmed by the direct application of ET during the infection of wheat and barley, which lead to increased susceptibility to *Fg*. Based on these findings, we suggest that negative regulators of ET are efficient targets for sRNA-directed manipulation of host immunity by *Fg*.

The bacterial pathogen *Pseudomonas syringae* secretes two effector molecules, AvrPto and AvrPtoB, into host plants. These effectors interact with the receptor-like kinase BRI1-associated receptor kinase 1 (BAK1), also known as SERK3, thereby preventing the recognition of various MAMPs through the association of BAK1 with pattern recognition receptors (PRRs) such as flagellin-sensitive 2 (FLS2) and Ef-Tu receptor (EFR) (Shan et al. 2008). We observed

390 *FgDCL*-dependent silencing of the cereal BAK1 homologs *HvBAK1*, *HvSERK2* and *BdSERK2*.
391 While these genes have a higher similarity to *AtSERK2* than to *AtSERK3* (*AtBAK1*), they still
392 are among the closest homologs to *AtBAK1* found in cereals (Fig. S9). It is tempting to speculate
393 that further experiments will uncover additional hubs that are targeted both by protein and
394 sRNA effectors.

395

396 **Conclusion**

397

398 Our data show that in the necrotrophic ascomycete *Fusarium graminearum* gene silencing by
399 RNAi shapes its ability to cause disease, which is consistent with earlier results on the
400 significance of the RNAi machinery in *Fg* (Gaffar et al. 2019; Son et al. 2017). Pathogenicity
401 relies on DICER-like (DCL)-dependent sRNAs that were identified as potential candidates for
402 fungal effectors targeting defence genes in two Poaceae hosts, barley and *Brachypodium*. We
403 identified *Fg*-sRNAs with sequence homology to host genes that were down-regulated by *Fg*
404 during plant colonisation, while they were expressed above their level in healthy plants after
405 infection with a DCL dKO mutant. In PH1-*dcl1/2 vs*. PH1 the strength of target gene
406 accumulation correlated with the abundance of the corresponding *Fg*-sRNA. Our data hint to
407 the possibility that three DCL-dependent tRFs with sequence homology to immunity-related
408 *Ethylene overproducer 1-like 1* (*HvEOL1)* and three Poaceae orthologues of *Arabidopsis*
409 *thaliana BRI1-associated receptor kinase 1* (*HvBAK1, HvSERK2* and *BdSERK2*) contribute to
410 fungal virulence via targeted gene silencing.

411

Experimental procedures

Plants, fungi and plant infection

Fusarium graminearum (*Fg*) strain PH1, the double knock-out (dKO) PH1-*dcl1/2* (Dr. Martin Urban, Rothamsted Research, England), strain IFA65 (IFA, Department for Agrobiotechnology, Tulln, Austria) and single mutants IFA65-*dcl1* and IFA65-*dcl2* (Gaffar et al. 2019) were cultured on synthetic nutrient poor agar (SNA). Preparation of fungal inoculum was performed as described (Koch et al. 2013). *Arabidopsis thaliana* ecotype Col-0 and *Atago1-27* (Morel et al. 2002; Polymorphism:3510706481) were grown in 8 h photoperiod at 22°C with 60% relative humidity in a soil - sand mixture (4:1) (Fruhstorfer Type T, Hawita, Germany). For infection, 15 rosette leaves were detached and transferred in square Petri plates containing 1% water-agar. Drop-inoculation of Arabidopsis leaves was done with 5 µl of a suspension of 5×10^4 *Fg* conidia ml^{-1} at two spots per leaf. Infection strength was recorded as infection area (size of chlorotic lesions relative to total leaf area) using the ImageJ software (https://imagej.nih.gov/ij/).

For infection of barley (*Hordeum vulgare* cv. Golden Promise, GP) and *Brachypodium distachyon* (Bd21-3), plants were grown in a 16 h photoperiod at 20°C/18°C day/night and 60% relative humidity in soil (Fruhstorfer Type LD80, Hawita). Ten detached second leaves were transferred into square Petri plates containing 1% water-agar. GP leaves were drop-inoculated with 3 µl of 1.5 x 10^5 conidia ml^{-1} conidia suspension. Bd21-3 leaves were drop-inoculated on two spots with 10 µl of 1 x 10^4 conidia ml^{-1} conidia suspension. Infection strength was measured with the PlantCV v2 software package (https://plantcv.danforthcenter.org/) by training a machine learning algorithm to recognize necrotic lesions. For gene expression analysis, a suspension of 5 x 10^4 *Fg* conidia ml^{-1} was used and leaves were either inoculated on 3 spots with 20 µl (barley) or on 2 spots with 10 µl (Brachypodium), respectively and experiments were evaluated 5 days post inoculation (dpi).

Fungal transcript analysis

Gene expression analysis was performed using reverse transcription quantitative PCR (RT-qPCR). RNA extraction was performed with GENEzol reagent (Geneaid) following the manufacturer's instructions. Freshly extracted mRNA was used for cDNA synthesis using qScript™ cDNA kit (Quantabio). For RT-qPCR, 10 ng of cDNA was used as template in the QuantStudio 5 Real-Time PCR system (Applied Biosystems). Amplifications were performed with 5 µl of SYBR® green JumpStart Taq ReadyMix (Sigma-Aldrich) with 5 pmol oligonucleotides. Each sample had three technical repetitions. After an initial activation step at 95°C for 5 min, 40 cycles (95°C for 30 sec, 60°C for 30 sec, 72°C for 30 sec) were performed followed by a melt curve analysis (60°C-95°C, 0.075°C/s). Ct values were determined with the QuantStudio design and analysis software supplied with the instrument. Transcript levels were determined via the $2^{-\Delta\Delta Ct}$ method (Livak & Schmittgen 2001) by normalizing the amount of target transcript to the amount of the reference transcript *Elongation factor 1-alpha* (*EF1-a*, FGSG_08811) gene (Tab. S1).

Plant transcript analysis

Leaves were shock frozen at 5 dpi and RT-qPCR was performed as described above. Reference genes were *Ubiquitin-40S ribosomal protein S27a-3* (HORVU1Hr1G023660) for GP and *Ubi4* (Bradi3g04730) for Bd21-3 according to Chambers et al. (2012) (Tab. S1). Primers were designed using Primer3 v2.4.0 (Untergasser et al. 2012).

Spray application of dsRNA

Second leaves of 2 to 3-week-old GP were detached and transferred to square Petri plates containing 1% water agar. dsRNA was diluted in 500 µl water to a final concentration of 20 ng μl^{-1}. As control, Tris-EDTA (TE) buffer was diluted in 500 µl water corresponding to the amount used for dilution of the dsRNA. Typical RNA concentration after elution was 500 ng/µl,

461 with 400 µM Tris-HCL and 40 µM EDTA in the final dilution. Each plate containing 10
462 detached leaves was evenly sprayed with either dsRNAs or TE buffer with 500 µl, and
463 subsequently kept at room temperature (Koch et al. 2016). Two days after spraying, leaves were
464 drop-inoculated with three 20 µl drops of *Fg* suspension containing 5×10^4 conidia ml^{-1}. After
465 inoculation, plates were closed and incubated for five days at room temperature.

466 ***Target prediction for sRNAs***

467 RNA was purified and enriched for sRNAs from fungal axenic culture using the mirVana
468 miRNA Isolation Kit (Life Technologies). Indexed sRNA libraries were constructed from these
469 sRNA fractions with the NEBNext Multiplex Small RNA Library Prep Set for Illumina (New
470 England Biolabs) according to the manufacturer's instructions. Reads were trimmed with the
471 cutadapt tool v2.1 (Martin 2011) by removing adapters and retaining reads with a length of 21-
472 24 nt and quality checked with the fastQC tool v0.11.9
473 (http://www.bioinformatics.babraham.ac.uk/projects/fastqc/). For Fig. S1 reads were aligned to
474 the *Fg* reference genome (GCF_000240135.3_ASM24013v3) with bowtie2 (Langmead &
475 Salzberg 2012) following a sensitive alignment policy (-D 100, -R 10, -L 19). The aligned reads
476 were assigned to the additional attribute "gene_biotype" with htseq-count (Anders et al. 2015)
477 according to the latest assembly (ftp://ftp.ensemblgenomes.org/pub/release-
478 44/fungi/gff3/fungi_ascomycota3_collection/fusarium_graminearum_gca_000240135).
479 Remaining reads were collapsed with the fastx toolkit v0.0.14 (Hannon 2010) and reads with
480 at least 400 reads were targeted against the IBSC_PGSB_v2 cDNA annotation with the plant
481 miRNA target prediction algorithm TAPIR (Bonnet et al. 2010), following the optimized
482 parameters according to Srivastava et al. (2014). The results of the target prediction were further
483 analysed with RStudio (RStudio Team 2016) and the package biomaRt (Durinck et al. 2005) to
484 find targets associated with stress and immunity associated Gene ontology (GO) terms in the
485 database "plants_mart" from plants.ensembl.org hosted by the EBI (European Bioinformatics

Institute) and the Wellcome Trust Sanger Institute. The same method was used for the identification of target genes in *B. distachyon* (GCA_000005505.4) and *A. thaliana* (Araport11).

Stemloop-RT-qPCR of sRNAs

RNA was extracted and genomic DNA was digested as described above. The sequences of sRNAs found in axenic fungal culture were used to design specific stem loop (SL) primers matching the sRNA over 6 nt at the 3'end. For the primer design, the tool of Adhikari et al. (2013) was used. SL-primers were diluted to 10 pM and folded in a cycler (95°C for 15 min, 90°C 5 min, 85°C 5 min, 80°C 5 min, 75°C 1 h, 68°C 1 h, 65°C 1 h, 62°C 1 h, 60°C 3 h). These primers were used for cDNA synthesis (Thermo Scientific RevertAid RT Reverse Transcription Kit) according to manufacturer's instruction with an annealing step at 16°C instead of 25°C and were used in multiplex to target respective fungal sRNAs and barley miRNAs *Hvu*-mir159 and *Hvu*-mir168 as references. To obtain amplification efficiencies, a mix from all RNAs was diluted in a four step dilution series with a factor of ten and reverse transcribed. Reactions were set up with the highest concentration of 15 ng μl^{-1} and the lowest of 15 pg μl^{-1} cDNA. All sRNA amplifications showed an efficiency of 80-82% and an R^2 between 1 and 0.997 except for Fg-sRNA-6717 with an efficiency of 66.4%. For RT-qPCR, 1.5 µl of 3 ng μl^{-1} cDNA was used as template in the QuantStudio 5 Real-Time PCR system (Applied Biosystems). Amplifications were performed with 5 µl of SYBR® green JumpStart Taq ReadyMix (Sigma-Aldrich) with 1.5 pmol or 3 pmol oligonucleotides. Each sample had three technical repetitions. As forward primer the unused nucleotides of the remaining sequence of the sRNA were used, which were extended to achieve optimal melting temperature, and as reverse primer the universal stem loop primer developed by Chen et al. (2005) was used. Relative abundance of the sRNAs was calculated with the ΔΔct-method with incorporation of amplification efficiencies. sRNAs were

510 normalized against the reference miRNAs Hvu-mir-159a and 168-5p and after this against the
511 fungal biomass measured as *EF1-α* against *HvUBQ* (*HORVU1Hr1G023660*).

512 ***Statistics***

513 To assess the differential expression of genes via RT-qPCRs the Δct values were compared via
514 a one or two sided paired Students *t*-test. Disease symptoms were either compared via Students
515 *t*-test if the data showed a normal distribution in Shapiro-Wilk test or via a Wilcoxon rank sum
516 test.

517 ***RLM-RACE***

518 RNA from GP barley infected with *Fg*-IFA65 at 5 dpi and an uninfected control was extracted
519 with the Isolate II plant miRNA kit (Bioline). 1 µg of RNA (>200 nt) of infected, uninfected
520 and a mix of both samples for a –RT-control were assembled. 1 µl of the 5'RACE Adapter [0.3
521 µg/µl], 1 µl of the 10x Reaction Buffer, 1 µl of 1mg/µl BSA, 0.5 µl of T4 RNA Ligase [10U/µl]
522 (Thermo Scientific) and DEPC-treated water up to 10 µl were prepared and incubated at 37°C
523 for 60 min. Subsequently, the whole reaction was used for reverse transcription (RevertAid
524 Reverse Transcriptase, Thermo Scientific). 10 µl ligation reaction, 1 µl Random Hexamer
525 [100pmol/µl], 4 µl 5x Reaction Buffer, 0.5 µl RiboLock RNase Inhibitor (Thermo Scientific),
526 2 µl dNTP Mix [10 mM] and 1 µl RevertAid Reverse Transcriptase (or water (–RT control))
527 and 1.5 µl water were mixed and run for 10 min at 25°C, 60 min at 42°C and 10 min at 70°C.
528 Then, a nested hot-start touch-down PCR for each target gene was performed. The primer
529 sequences for the outer (first) and inner (second) PCR are shown in Tab. S1. 5 µl of 10x Buffer
530 B, 1 µl of a dNTP Mix [10 mM], 2 µl $MgCl_2$ [25 mM], 1µl Adapter specific Primer [10 pmol
531 μl^{-1}] and 1 µl gene specific primer (GSP) [10 pmol μl^{-1}], 0.6 µl DCS DNA Polymerase (DNA
532 Cloning Service) [5 U/µl] and 2 µl cDNA or outer PCR reaction and 37.4 µl water were mixed
533 and run at 95°C for 5 min, (95°for 30 s, 68°C-0.5°C/cycle for 30 s, 72°C for 30 s)*15, (95°C
534 for 30 s, 60°C for 30 s, 72°C for 30 s)*18 and 72°C for 5 min. PCR products were evaluated in

a 1.5% agarose gel and bands of the expected size, which were present in the infected but not uninfected samples, were excised. Products were cleaned with the Wizard SV Gel and PCR Clean-Up System (Promega) and cloned with the pGEM-T easy Vector Systems (Promega). For each band, five clones were picked for sequencing. Plasmids from O/N cultures were extracted with the Monarch Plasmid Miniprep Kit (New England Biolabs) and sent for sequencing to LGC genomics.

Analysis of target genes and targeting sRNAs

After the initial target prediction an additional target prediction for the newly released cultivar specific genome (GCA_902500625) of barley cv. Golden Promise (GP) was conducted. Adapters were removed and reads were collapsed as described before for the target prediction. All sRNA sequences were read with SeqinR (v3.6-1; Charif & Lobry 2007) and stored in a list of SeqFastadna objects. To identify the homologous genes to the already identified targets in GP, the cDNA library was blasted with the command-line blast application (Nucleotide-Nucleotide BLAST 2.6.0+) (Camacho et al. 2009) against the identified target sequences from the IBSC_PGSB_v2 cDNA library with percent identity of 90 and a query coverage of 55% as cut-off values. All sRNAs with at least two reads were written to a file in chunks of 2000 each and ran against each individual target gene with TAPIR via the system2 function in R (R Core Team 2019) in the RStudio software. Results were collected, stored in a data.frame, and further analysed with R. sRNAs identified to target a gene of interest (GOI) were written to a fasta file with SeqinR and blasted against the rRNAs from the assemblies GCA_900044135.1 (*Fg*-PH1), GCA_000240135.3 (*Fg*-PH1) and the Fusarium rRNAs from the RNAcentral fungal ncRNA dataset (ftp://ftp.ebi.ac.uk/pub/databases/RNAcentral/current_release/sequences/by-database/ensembl_fungi.fasta (12/Sep/2020)) with the options wordsize=4, perc_identity=95, qcov_hsp_perc=95. All sRNAs matching rRNAs were removed. Thereafter, sRNAs were

559 compared to the *Fg* assemblies GCA_900044135.1 (*Fg*-PH1) and GCA_000240135.3 (*Fg*-
560 PH1) with the same blast strategy and only perfectly matching sRNAs were retained.

561 To derive the relative expression of a GOI between two samples the following formula is used.

562 $$Relativeexpression_{GOI} = 2^{-\Delta\Delta ct_{GOI}}$$

563 We further defined the ΔΔΔct value as the difference between the ΔΔct values for a GOI in PH1
564 and PH1-*dcl1/2*-infected samples.

565 $$\Delta\Delta\Delta\text{ct} = \Delta\Delta ct_{PH1-dcl1/2} - \Delta\Delta ct_{PH1}$$

566 This enables the calculation of the re-accumulation between the two samples as follows.

567 $$DCL\text{-}dependent\ resurgence\ \ factor = \frac{Relativeexpression_{PH1-dcl1/2}}{Relativeexpression_{PH1}} = 2^{-\Delta\Delta\Delta ct_{GOI}}$$

568

569 The sum of all reads and the corresponding ΔΔΔct-value were plotted with ggplot2 (Wickham
570 2016) and a linear regression was added to the plot. To allow a log2-transformation of the plots
571 genes with zero targeting reads were set to one targeting read. The plots were arranged using
572 ggpubr v.0.4.0 (Kassambara 2017).

573 ***GO enrichment analysis***

574 Gene ontology (GO) enrichment analysis was performed via the AgriGO v.2.0 analysis toolkit
575 (Tian 2017) with the standard parameters singular enrichment analysis (SEA).

576 ***Phylogenetic analysis of SERK homologs***

577 Homologs of *HvBAK1* and *HvSERK2* were searched in *At*, *Hv* and *Bd* with biomaRt v.2.40.5
578 (Durinck et al. 2005) and downloaded from the EMBL's European Bioinformatics Institute
579 plants genome page (plants.ensembl.org) in the plants_mart dataset hvulgare_eg_gene
580 (Ensembl Plants Genes v. 50). For these homologs the CDS of all homologs within the

581 respective datasets athaliana_eg_gene, hvulgare_eg_gene and bdistachyon_eg_gene were
582 downloaded. The CDS were subsequently aligned with the muscle algorithm in MEGA7
583 (Kumar et al. 2016b) and a phylogenetic tree was constructed via a bootstrap method with 200
584 iterations.

585 ***Acknowledgements***

586 We thank the Salk Institute Genomic Analysis Laboratory for providing the sequence-indexed

587 Arabidopsis TDNA insertion mutants. This work was supported by the Deutsche

588 Forschungsgemeinschaft (Research Unit FOR5116) to KHK.

589

Supporting Information

Fig. S1: Feature mapping of Fg-sRNAs with a read length of 21-24 nt

Reads were trimmed as described earlier and aligned to the PH1 reference genome (GCF_000240135.3_ASM24013v3) with bowtie2 (Langmead & Salzberg 2012).

Fig. S2: GO-enrichment analysis of all potential targets of Fg-sRNAs with more than 400 reads

The plot shows all significantly enriched GO-terms in the target gene set for (A) molecular function and (B) biological process. The analysis was done using agriGo v2.0. Each box contains information regarding one term. GO: indicates the GO accession, in brackets the p-value is stated (Fisher; Yekutieli (FDR)). After the bracket the GO-term description is written followed by the number of genes associated with said term 1. in the gene set and 2. In the background.

Fig. S3: Alignment of AtETO1 and HvEOL1

Identical amino acids are marked blue and similar amino acids are marked red. The alignment and visualization was done with the msa package for R (Bodenhofer et al. 2015).

Fig. S4: Regulation of ET synthesis in At

*At*ETO1 negatively regulates ethylene **(ET)** synthesis in *At***.** *At*ETO1 acts together with *At*EOL1 and *At*ETO1-like 2 (EOL2) in directing the ubiquitination and subsequent degradation of type-2 1-aminocyclopropane-1-carboxylate synthase (ACS) proteins (e.g. ET overproducer 2 (ETO2)), which produce the direct precursor of ET.

Fig S5: Sequences of dsRNA-dcl1/2

611 Coding Sequences (CDS) of the respective *FgDCL* genes with the sequences comprising the
612 dsRNAs marked in red. **A.** *FgDCL1*-FGSG_09025 (912 nt long dsRNA-*Fg*DCL1). **B.**
613 *FgDCL2*-FGSG_04408 (870 nt long dsRNA-*Fg*DCL2).

614 ***Fig. S6: Position and read count of all tRFs from Fg-tRNA-Gly(GCC)***

615 Alignment position of all *Fg*-sRNAs from axenic culture with more than 50 reads perfectly
616 matching the *Fg*-tRNA-Gly(GCC)-9 gene (Fusarium_graminearum_CS3005-tRNA-Gly-GCC-
617 1-9) colored by read count.

618 ***Fig. S7: Abundance of unique Fg-sRNAs in axenic culture of IFA65***

619 A: Histogram of the read count of every unique sRNA. The plot is truncated to make
620 abundances recognizable. Most sRNAs have very low read counts and very few sRNAs have
621 more reads than 3,000. Maximum read count per sRNA is 42,866. B: Violin plot of log2-
622 transformed reads counts untruncated.

623 ***Fig. S8: Origin of tRFs in Fg-tRNA-Gly(GCC)***

624 The centroid secondary structure of the *Fg*-tRNA-Gly(GCC) generated on the RNAfold web
625 server (http://rna.tbi.univie.ac.at/cgi-bin/RNAWebSuite/RNAfold.cgi) with the origin and
626 alignment of *Fg*-sRNA-321, *Fg*-sRNA-1921 and *Fg*-sRNA-6717. The colors of bases indicate
627 the base pair probabilities.

628 ***Fig. S9: Molecular Phylogenetic analysis by Maximum Likelihood method***

629 The evolutionary history was inferred by using the Maximum Likelihood method based on the
630 General Time Reversible model (Nei & Kumar, 2000). The tree with the highest log likelihood
631 (-25430.37) is shown. Initial tree(s) for the heuristic search were obtained automatically by
632 applying Neighbor-Join and BioNJ algorithms to a matrix of pairwise distances estimated using
633 the Maximum Composite Likelihood (MCL) approach, and then selecting the topology with
634 superior log likelihood value. The tree is drawn to scale, with branch lengths measured in the

635 number of substitutions per site. The analysis involved 77 nucleotide sequences. Codon
636 positions included were 1st+2nd+3rd. There were a total of 2427 positions in the final dataset.
637 Evolutionary analyses were conducted in MEGA7 (Kumar et al. 2016b).

638 ***Tab. S1: Primer sequences***

639 Sequences and target accessions for all primers used in the study

640 ***Tab. S2: Target prediction results***

641 Results of the target prediction with the TAPIR algorithm for all *Fg*-sRNAs with more than 400
642 reads

643

644

References

Abeles, F. W. (1992). Roles and physiological effects of ethylene in plant physiology: dormancy, growth, and development. *Ethylene in plant biology*.

Adhikari, S., Turner, M., & Subramanian, S. (2013). Hairpin priming is better suited than in vitro polyadenylation to generate cDNA for plant miRNA qPCR. *Molecular plant*, *6*(1), 229-231.

Alonso, J. M., Hirayama, T., Roman, G., Nourizadeh, S., & Ecker, J. R. (1999). EIN2, a bifunctional transducer of ethylene and stress responses in Arabidopsis. *Science*, *284*(5423), 2148-2152.

Anders, S., Pyl, P. T., & Huber, W. (2015). HTSeq—a Python framework to work with high-throughput sequencing data. *Bioinformatics*, *31*(2), 166-169.

Asha, S., & Soniya, E. V. (2016). Transfer RNA derived small RNAs targeting defense responsive genes are induced during Phytophthora capsici infection in black pepper (Piper nigrum L.). *Frontiers in plant science*, *7*, 767.

Åsman, A. K., Vetukuri, R. R., Jahan, S. N., Fogelqvist, J., Corcoran, P., Avrova, A. O., ... & Dixelius, C. (2014). Fragmentation of tRNA in Phytophthora infestans asexual life cycle stages and during host plant infection. *BMC microbiology*, *14*(1), 308.

Bodenhofer, U., Bonatesta, E., Horejš-Kainrath, C., & Hochreiter, S. (2015). msa: an R package for multiple sequence alignment. *Bioinformatics*, *31*(24), 3997-3999.

Bonnet, E., He, Y., Billiau, K., & Van de Peer, Y. (2010). TAPIR, a web server for the prediction of plant microRNA targets, including target mimics. *Bioinformatics*, *26*(12), 1566-1568.

667 Cai, Q., He, B., Kogel, K. H., & Jin, H. (2018a). Cross-kingdom RNA trafficking and
668 environmental RNAi—nature's blueprint for modern crop protection strategies. *Current*
669 *opinion in microbiology*, *46*, 58-64.

670 Cai, Q., Qiao, L., Wang, M., He, B., Lin, F. M., Palmquist, J., ... & Jin, H. (2018b). Plants send
671 small RNAs in extracellular vesicles to fungal pathogen to silence virulence genes. *Science*,
672 *360*(6393), 1126-1129.

673 Camacho, C., Coulouris, G., Avagyan, V., Ma, N., Papadopoulos, J., Bealer, K., & Madden, T.
674 L. (2009). BLAST+: architecture and applications. *BMC bioinformatics*, *10*(1), 1-9.

675 Chambers, J. P., Behpouri, A., Bird, A., & Ng, C. K. (2012). Evaluation of the use of the
676 Polyubiquitin Genes, Ubi4 and Ubi10 as reference genes for expression studies in
677 Brachypodium distachyon. *PLoS One*, *7*(11), e49372.

678 Charif, D., & Lobry, J. R. (2007). SeqinR 1.0-2: a contributed package to the R project for
679 statistical computing devoted to biological sequences retrieval and analysis. In *Structural*
680 *approaches to sequence evolution* (pp. 207-232). Springer, Berlin, Heidelberg.

681 Chen, C., Ridzon, D. A., Broomer, A. J., Zhou, Z., Lee, D. H., Nguyen, J. T., ... & Guegler, K.
682 J. (2005). Real-time quantification of microRNAs by stem–loop RT–PCR. *Nucleic acids*
683 *research*, *33*(20), e179-e179.

684 Chen, X., Steed, A., Travella, S., Keller, B., & Nicholson, P. (2009). Fusarium graminearum
685 exploits ethylene signalling to colonize dicotyledonous and monocotyledonous plants. *New*
686 *Phytologist*, *182*(4), 975-983.

687 Christians, M. J., Gingerich, D. J., Hansen, M., Binder, B. M., Kieber, J. J., & Vierstra, R. D.
688 (2009). The BTB ubiquitin ligases ETO1, EOL1 and EOL2 act collectively to regulate ethylene
689 biosynthesis in Arabidopsis by controlling type-2 ACC synthase levels. *The Plant Journal*,
690 *57*(2), 332-345.

691 Curaba, J., Spriggs, A., Taylor, J., Li, Z., & Helliwell, C. (2012). miRNA regulation in the early
692 development of barley seed. *BMC plant biology*, *12*(1), 1-16.

693 Dean, R., Van Kan, J. A., Pretorius, Z. A., Hammond-Kosack, K. E., Di Pietro, A., Spanu, P.
694 D., ... & Foster, G. D. (2012). The Top 10 fungal pathogens in molecular plant pathology.
695 *Molecular plant pathology*, *13*(4), 414-430.

696 Deng, P., Wang, L., Cui, L., Feng, K., Liu, F., Du, X., ... & Weining, S. (2015). Global
697 identification of microRNAs and their targets in barley under salinity stress. *PLoS One*, *10*(9),
698 e0137990.

699 Desjardins, A. E., Hohn, T. M., & McCORMICK, S. P. (1993). Trichothecene biosynthesis in
700 Fusarium species: chemistry, genetics, and significance. *Microbiology and Molecular Biology*
701 *Reviews*, *57*(3), 595-604.

702 Dubey, H., Kiran, K., Jaswal, R., Jain, P., Kayastha, A. M., Bhardwaj, S. C., ... & Sharma, T.
703 R. (2019). Discovery and profiling of small RNAs from Puccinia triticina by deep sequencing
704 and identification of their potential targets in wheat. *Functional & integrative genomics*, *19*(3),
705 391-407.

706 Dunker, F., Trutzenberg, A., Rothenpieler, J. S., Kuhn, S., Pröls, R., Schreiber, T., ... &
707 Weiberg, A. (2020). Oomycete small RNAs bind to the plant RNA-induced silencing complex
708 for virulence. *Elife*, *9*, e56096.

709 Durinck, S., Moreau, Y., Kasprzyk, A., Davis, S., De Moor, B., Brazma, A., & Huber, W.
710 (2005). BioMart and Bioconductor: a powerful link between biological databases and
711 microarray data analysis. *Bioinformatics*, *21*(16), 3439-3440.

712 Ferdous, J., Sanchez-Ferrero, J. C., Langridge, P., Milne, L., Chowdhury, J., Brien, C., &
713 Gaffar, F. Y., & Koch, A. (2019). Catch me if you can! RNA silencing-based improvement of
714 antiviral plant immunity. *Viruses*, *11*(7), 673.

715 Gaffar FY, Imani J, Karlovsky P, Koch A, Kogel KH (2019) Different components of the RNAi
716 machinery are required for conidiation, ascosporogenesis, virulence, DON production and
717 fungal inhibition by exogenous dsRNA in the Head Blight pathogen *Fusarium graminearum*.
718 *Front. Microbiol* doi: 10.3389/fmicb.2019.01662.

719 Garcia-Silva, M. R., Cabrera-Cabrera, F., Cura das Neves, R. F., Souto-Padrón, T., de Souza,
720 W., & Cayota, A. (2014). Gene expression changes induced by Trypanosoma cruzi shed
721 microvesicles in mammalian host cells: relevance of tRNA-derived halves. *BioMed research*
722 *international*, *2014*.

723 Glazebrook, J. (2005). Contrasting mechanisms of defense against biotrophic and necrotrophic
724 pathogens. *Annu. Rev. Phytopathol.*, *43*, 205-227.

725 Guo, Q., Liu, Q., Smith, N.A., Liang, G., & Wang, M.B. (2016). RNA Silencing in plants:
726 mechanisms, technologies and applications in horticultural crops. *Current Genomics*, 17, 476–
727 489.

728 Hannon, G. "Fastx-toolkit." FASTQ/A Short-reads Preprocessing Tools (2010)

729 Hackenberg, M., Gustafson, P., Langridge, P., & Shi, B. J. (2015). Differential expression of
730 micro RNA s and other small RNA s in barley between water and drought conditions. *Plant*
731 *biotechnology journal*, *13*(1), 2-13.

732 Head, G. P., Carroll, M. W., Evans, S. P., Rule, D. M., Willse, A. R., Clark, T. L., ... & Meinke,
733 L. J. (2017). Evaluation of SmartStax and SmartStax PRO maize against western corn rootworm
734 and northern corn rootworm: efficacy and resistance management. *Pest management science*,
735 *73*(9), 1883-1899.

736 Ilgen, P., Hadeler, B., Maier, F. J., & Schäfer, W. (2009). Developing kernel and rachis node
737 induce the trichothecene pathway of Fusarium graminearum during wheat head infection.
738 *Molecular plant-microbe interactions*, *22*(8), 899-908.

739 Jansen, C., Von Wettstein, D., Schäfer, W., Kogel, K. H., Felk, A., & Maier, F. J. (2005).
740 Infection patterns in barley and wheat spikes inoculated with wild-type and trichodiene synthase
741 gene disrupted Fusarium graminearum. *Proceedings of the National Academy of Sciences*,
742 *102*(46), 16892-16897.

743 Jones-Rhoades, M. W. (2012). Conservation and divergence in plant microRNAs. *Plant*
744 *molecular biology*, *80*(1), 3-16.

745 Kaldis, A., Berbati, M., Melita, O., Reppa, C., Holeva, M., Otten, P., & Voloudakis, A. (2018).
746 Exogenously applied dsRNA molecules deriving from the Zucchini yellow mosaic virus
747 (ZYMV) genome move systemically and protect cucurbits against ZYMV. *Molecular plant*
748 *pathology*, *19*(4), 883-895.

749 Kassambara, A. (2017). ggpubr: "ggplot2" based publication ready plots. R package version
750 0.1. 6.

751 Kieber, J. J., Rothenberg, M., Roman, G., Feldmann, K. A., & Ecker, J. R. (1993). CTR1, a
752 negative regulator of the ethylene response pathway in Arabidopsis, encodes a member of the
753 raf family of protein kinases. *Cell*, *72*(3), 427-441.

754 Kim, H. K., Jo, S. M., Kim, G. Y., Kim, D. W., Kim, Y. K., & Yun, S. H. (2015). A large-scale
755 functional analysis of putative target genes of mating-type loci provides insight into the
756 regulation of sexual development of the cereal pathogen Fusarium graminearum. *PLoS Genet*,
757 *11*(9), e1005486.

758 Koch, A., Biedenkopf, D., Furch, A., Weber, L., Rossbach, O., Abdellatef, E., ... & Kogel, K.
759 H. (2016). An RNAi-based control of Fusarium graminearum infections through spraying of
760 long dsRNAs involves a plant passage and is controlled by the fungal silencing machinery.
761 *PLoS pathogens*, *12*(10), e1005901.

762 Koch, A., & Kogel, K. H. (2014). New wind in the sails: improving the agronomic value of
763 crop plants through RNA i-mediated gene silencing. *Plant biotechnology journal*, *12*(7), 821-
764 831.

765 Koch, A., Kumar, N., Weber, L., Keller, H., Imani, J., & Kogel, K. H. (2013). Host-induced
766 gene silencing of cytochrome P450 lanosterol C14α-demethylase–encoding genes confers
767 strong resistance to Fusarium species. *Proceedings of the National Academy of Sciences*,
768 *110*(48), 19324-19329.

769 Koch, A., & Wassenegger, M. (2021). Host-induced gene silencing–mechanisms and
770 applications. *New Phytologist* doi: 10.1111/nph.17364.

771 Konakalla, N. C., Kaldis, A., Berbati, M., Masarapu, H., & Voloudakis, A. E. (2016).
772 Exogenous application of double-stranded RNA molecules from TMV p126 and CP genes
773 confers resistance against TMV in tobacco. *Planta*, *244*(4), 961-969.

774 Kumar, P., Kuscu, C., & Dutta, A. (2016a). Biogenesis and function of transfer RNA-related
775 fragments (tRFs). *Trends in biochemical sciences*, *41*(8), 679-689.

776 Kumar, S., Stecher, G., & Tamura, K. (2016b). MEGA7: molecular evolutionary genetics
777 analysis version 7.0 for bigger datasets. *Molecular biology and evolution*, *33*(7), 1870-1874.

778 Langmead, B., & Salzberg, S. L. (2012). Fast gapped-read alignment with Bowtie 2. *Nature*
779 *methods*, *9*(4), 357.

780 Lax, C., Tahiri, G., Patiño-Medina, J. A., Cánovas-Márquez, J. T., Pérez-Ruiz, J. A., Osorio-
781 Concepción, M., ... & Calo, S. (2020). The Evolutionary Significance of RNAi in the Fungal
782 Kingdom. *International Journal of Molecular Sciences, 21*(24), 9348.

783 Lee Marzano, S. Y., Neupane, A., Mochama, P., Feng, C., & Saleem, H. (2019). Roles of
784 argonautes and dicers on Sclerotinia sclerotiorum antiviral RNA silencing. *Frontiers in Plant*
785 *Science*, *10*, 976.

786 Li, N., Han, X., Feng, D., Yuan, D., & Huang, L. J. (2019). Signaling crosstalk between salicylic
787 acid and ethylene/jasmonate in plant defense: do we understand what they are whispering?.
788 *International Journal of Molecular Sciences*, *20*(3), 671.

789 Li, N., Shan, N., Lu, L., & Wang, Z. (2021). tRFtarget: a database for transfer RNA-derived
790 fragment targets. *Nucleic Acids Research, 49*(D1), D254-D260.

791 Liu, S., Jaouannet, M., Dempsey, D. M. A., Imani, J., Coustau, C., & Kogel, K. H. (2020).
792 RNA-based technologies for insect control in plant production. *Biotechnology advances*, *39*,
793 107463.

794 Livak, K. J., & Schmittgen, T. D. (2001). Analysis of relative gene expression data using real-
795 time quantitative PCR and the 2− ΔΔCT method. *methods*, *25*(4), 402-408.

796 Mallory, A. C., Reinhart, B. J., Jones-Rhoades, M. W., Tang, G., Zamore, P. D., Barton, M. K.,
797 & Bartel, D. P. (2004). MicroRNA control of PHABULOSA in leaf development: importance
798 of pairing to the microRNA 5′ region. *The EMBO journal*, *23*(16), 3356-3364.

799 Martin, M. (2011). Cutadapt removes adapter sequences from high-throughput sequencing
800 reads. *EMBnet. journal*, *17*(1), 10-12.

801 Martinez, G., Choudury, S. G., & Slotkin, R. K. (2017). tRNA-derived small RNAs target
802 transposable element transcripts. *Nucleic acids research*, *45*(9), 5142-5152.

803 Mascher, M., Gundlach, H., Himmelbach, A., Beier, S., Twardziok, S. O., Wicker, T., ... &
804 Stein, N. (2017). A chromosome conformation capture ordered sequence of the barley genome.
805 *Nature*, *544*(7651), 427-433.

806 McLoughlin, A. G., Wytinck, N., Walker, P. L., Girard, I. J., Rashid, K. Y., de Kievit, T., ... &
807 Belmonte, M. F. (2018). Identification and application of exogenous dsRNA confers plant
808 protection against Sclerotinia sclerotiorum and Botrytis cinerea. *Scientific Reports*, *8*(1), 1-14.

809 Mitter, N., Worrall, E. A., Robinson, K. E., Li, P., Jain, R. G., Taochy, C., ... & Xu, Z. P. (2017).
810 Clay nanosheets for topical delivery of RNAi for sustained protection against plant viruses.
811 *Nature plants*, *3*(2), 1-10.

812 Morel, J. B., Godon, C., Mourrain, P., Béclin, C., Boutet, S., Feuerbach, F., ... & Vaucheret, H.
813 (2002). Fertile hypomorphic ARGONAUTE (ago1) mutants impaired in post-transcriptional
814 gene silencing and virus resistance. *The Plant Cell*, *14*(3), 629-639.

815 Mueth, N. A., Ramachandran, S. R., & Hulbert, S. H. (2015). Small RNAs from the wheat
816 stripe rust fungus (Puccinia striiformis f. sp. tritici). *Bmc Genomics*, *16*(1), 1-16.

817 Nei, M., & Kumar, S. (2000). *Molecular evolution and phylogenetics*. Oxford university press.

818 Niehl, A., & Heinlein, M. (2019). Perception of double-stranded RNA in plant antiviral
819 immunity. *Molecular plant pathology*, *20*(9), 1203-1210.

820 Niehl, A., Soininen, M., Poranen, M. M., & Heinlein, M. (2018). Synthetic biology approach
821 for plant protection using ds RNA. *Plant biotechnology journal*, *16*(9), 1679-1687.

822 Nowara, D., Gay, A., Lacomme, C., Shaw, J., Ridout, C., Douchkov, D., ... & Schweizer, P.
823 (2010). HIGS: host-induced gene silencing in the obligate biotrophic fungal pathogen Blumeria
824 graminis. *The Plant Cell*, *22*(9), 3130-3141.

825 Potuschak, T., Lechner, E., Parmentier, Y., Yanagisawa, S., Grava, S., Koncz, C., & Genschik,
826 P. (2003). EIN3-dependent regulation of plant ethylene hormone signaling by two Arabidopsis
827 F box proteins: EBF1 and EBF2. *Cell*, *115*(6), 679-689.

828 R Core Team, R. (2019). R: A language and environment for statistical computing.

829 Reinhart, B. J., Weinstein, E. G., Rhoades, M. W., Bartel, B., & Bartel, D. P. (2002).
830 MicroRNAs in plants. *Genes & development*, *16*(13), 1616-1626.

831 Ren, B., Wang, X., Duan, J., & Ma, J. (2019). Rhizobial tRNA-derived small RNAs are signal
832 molecules regulating plant nodulation. *Science*, *365*(6456), 919-922.

833 Rosa, C., Kuo, Y. W., Wuriyanghan, H., & Falk, B. W. (2018). RNA interference mechanisms
834 and applications in plant pathology. *Annual review of phytopathology*, *56*, 581-610.

835 RStudio Team (2016). RStudio: Integrated Development for R. RStudioInc., Boston, MA URL
836 http://www.rstudio.com/.

837 Sang, H., & Kim, J. I. (2020). Advanced strategies to control plant pathogenic fungi by host-
838 induced gene silencing (HIGS) and spray-induced gene silencing (SIGS). *Plant Biotechnology*
839 *Reports*, *14*(1), 1-8.

840 Šečić E and Kogel KH (2021). Requirements for fungal uptake of dsRNA and gene silencing
841 in RNAi-based crop protection strategies. *Current Opinion in Biotechnology,* COBIOT-D-21-
842 00048.

843 Shan, L., He, P., Li, J., Heese, A., Peck, S. C., Nürnberger, T., ... & Sheen, J. (2008). Bacterial
844 effectors target the common signaling partner BAK1 to disrupt multiple MAMP receptor-
845 signaling complexes and impede plant immunity. *Cell host & microbe*, *4*(1), 17-27.

846 Son H, Park AR, Lim JY, Shin C, Lee Y-W (2017) Genome-wide exonic small interference
847 RNA-mediated gene silencing regulates sexual reproduction in the homothallic fungus
848 Fusarium graminearum. PLoS Genet 13(2): e1006595. doi:10.1371/journal.pgen.1006595

849 Srivastava, P. K., Moturu, T. R., Pandey, P., Baldwin, I. T., & Pandey, S. P. (2014). A
850 comparison of performance of plant miRNA target prediction tools and the characterization of
851 features for genome-wide target prediction. *BMC genomics*, *15*(1), 1-15.

852 Streit, R. S. A., Ferrareze, P. A. G., Vainstein, M. H., & Staats, C. C. (2021). Analysis of tRNA-
853 derived RNA fragments (tRFs) in Cryptococcus spp.: RNAi-independent generation and
854 possible compensatory effects in a RNAi-deficient genotype. *Fungal Biology*.

855 Tian, T., Liu, Y., Yan, H., You, Q., Yi, X., Du, Z., ... & Su, Z. (2017). agriGO v2. 0: a GO
856 analysis toolkit for the agricultural community, 2017 update. *Nucleic acids research*, *45*(W1),
857 W122-W129.

858 Untergasser, A., Cutcutache, I., Koressaar, T., Ye, J., Faircloth, B. C., Remm, M., & Rozen, S.
859 G. (2012). Primer3—new capabilities and interfaces. *Nucleic acids research, 40*(15), e115-
860 e115.

861 Wang, B., Sun, Y.F., Song, N., Zhao, M.X., Liu, R., Feng, H., Wang, X.J., & Kang, Z.S.
862 (2017a). *Puccinia striiformis f. sp tritici* microRNA-like RNA 1 (Pst-milR1), an important
863 pathogenicity factor of Pst, impairs wheat resistance to Pst by suppressing the wheat
864 pathogenesis-related 2 gene. *New Phytologist, 215*, 338–350.

865 Wang, M., Weiberg, A., Dellota, E. Jr, Yamane, D, & Jin, H. (2017b). Botrytis small RNA Bc-
866 siR37 suppresses plant defense genes by cross-kingdom RNAi. *RNA Biology, 14*, 421–428.

867 Wang, M., Weiberg, A., Lin, F.-M., Thomma, B. P. H. J., Huang, H.D., & Jin, H. (2016a).
868 Bidirectional cross-kingdom RNAi and fungal uptake of external RNAs confer plant protection.
869 *Nature Plants, 2*, 16151.

870 Wang, Q., Li, T., Xu, K., Zhang, W., Wang, X., Quan, J., ... & Shan, W. (2016b). The tRNA-
871 derived small RNAs regulate gene expression through triggering sequence-specific degradation
872 of target transcripts in the oomycete pathogen Phytophthora sojae. *Frontiers in plant science*,
873 *7*, 1938.

874 Weiberg, A., Wang, M., Lin, F. M., Zhao, H., Zhang, Z., Kaloshian, I., ... & Jin, H. (2013).
875 Fungal small RNAs suppress plant immunity by hijacking host RNA interference pathways.
876 *Science*, *342*(6154), 118-123.

877 Werner, B. T., Gaffar, F. Y., Schuemann, J., Biedenkopf, D., & Koch, A. M. (2020). RNA-
878 spray-mediated silencing of Fusarium graminearum AGO and DCL genes improve barley
879 disease resistance. *Frontiers in Plant Science*, *11*, 476.

880 Wickham, H. (2016). *ggplot2: elegant graphics for data analysis*. springer.

881 Yoshida, H., Wang, K.L., Chang, C.M., Mori, K., Uchida, E., Ecker, J.R. (2006). The ACC
882 synthase TOE sequence is required for interaction with ETO1 family proteins and
883 destabilization of target proteins. Plant Mol Biol. 62(3):427-37.

884 Zanini, S., Šečić, E., Busche, T., Galli, M., Zheng, Y., Kalinowski, J., & Kogel, K. H. (2021).
885 Comparative Analysis of Transcriptome and sRNAs Expression Patterns in the Brachypodium
886 distachyon—Magnaporthe oryzae Pathosystems. *International Journal of Molecular Sciences*,
887 *22*(2), 650.

888 Zuo, Y., Zhu, L., Guo, Z., Liu, W., Zhang, J., Zeng, Z., ... & Peng, Y. (2021). tsRBase: a
889 comprehensive database for expression and function of tsRNAs in multiple species. *Nucleic*
890 *Acids Research, 49*(D1), D1038-D1045.

891

892

Tables

Tab. 1: Selected GO-terms of tested genes and closest homologs in A. thaliana

Name	ensembl_gene_id	GO_term	*A.thaliana* Homolog	Abbr.
HvARF3 Auxin response transcription factor 3	HORVU1Hr1G076690	auxin-activated signaling pathway regulation of transcription, DNA-templated nucleus	AT2G33860	*ARF3*
HvSUB1 Short under blue light 1	HORVU2Hr1G028070	Golgi apparatus transferase activity, transferring glycosyl groups fucose metabolic process	AT4G08810	*SUB1*
HvPPR Pentatricopeptide repeat superfamily protein	HORVU2Hr1G078260	protein binding	AT2G06000	
HvSERK2 Somatic embryogenesis receptor-like kinase 2_1	HORVU2Hr1G080020	integral component of membrane positive regulation of innate immune response regulation of defense response to fungus	AT1G34210	*SERK2*
HvARF10 Auxin response transcription factor 10	HORVU2Hr1G089670	auxin-activated signaling pathway regulation of transcription, DNA-templated nucleus	AT2G28350	*ARF10*
HvEOL1 ETO1-like 1	HORVU2Hr1G119180	regulation of ethylene biosynthetic process protein binding	AT4G02680	*EOL1*
HvRST1 Resurrection 1	HORVU3Hr1G016630	integral component of membrane membrane	AT3G27670	*RST1*
HvPIX7 Putative interactor of XopAC 7	HORVU3Hr1G051080	protein serine/threonine kinase activity ATP binding protein kinase activity	AT5G15080	*PIX7*
Hvemb2726 Embryo defective 2726	HORVU5Hr1G024470	translation elongation factor activity mitochondrion intracellular	AT4G29060	*emb2726*
HvPGLP2 2-Phosphoglycolate phosphatase 2	HORVU5Hr1G052320	chloroplast phosphoglycolate phosphatase activity hydrolase activity	AT5G47760	*PGLP2*

HvATG2 Autophagy-related 2	HORVU6Hr1G034660	autophagy of peroxisome autophagy	AT3G19190	*ATG2*
HvSUVR5 Su(var)3-9-related protein 5	HORVU6Hr1G069350	histone-lysine N-methyltransferase activity chromosome methyltransferase activity	AT2G23740	*SUVR5*
HvRDR1 RNA-dependent RNA polymerase 1	HORVU6Hr1G074180	RNA-directed 5'-3' RNA polymerase activity RNA binding gene silencing by RNA	AT1G14790	*RDR1*
HvGDH Glycine decarboxylase complex H	HORVU6Hr1G076880	glycine decarboxylation via glycine cleavage system glycine cleavage complex mitochondrion	AT2G35370	*GDH1*
HvBAK1 Somatic embryogenesis receptor-like kinase 2_2	HORVU7Hr1G068990	integral component of membrane transmembrane receptor protein serine/threonine kinase signaling pathway	AT1G34210	*SERK2*
HvARF19 Auxin response transcription factor 19	HORVU7Hr1G096460	auxin-activated signaling pathway regulation of transcription, DNA-templated nucleus		
BdSERK2	BRADI_5g12227v3	integral component of membrane positive regulation of innate immune response regulation of defense response to fungus	AT1G34210	*SERK2*

qPCR and RT primer used in this study. First column shows the name of the respective template. Second column gives the accession for genes or the sequence of sRNAs. Third column shows the primer names and fourth column gives the oligonucleotide sequence. Lower case letters are complementary to the respective sRNA.

901

902 ***Tab. 2: Target prediction results of Fg-sRNAs with more than 400 reads in IFA65 axenic***

903 ***culture.***

sRNA-Name	Reads	Score	Alignment				Length
Fg-sRNA-321	2106	4.5	3'	GCUUGGGUCCCGAGGGGCUACC	5'		22
				..|.o|||||||||||o|||			
HvEOL1			5'	GAAUUCCAGGGCUCCCCGGUGG	3'		
Fg-sRNA-1921	416	3.5	3'	CUUGGGUCCCGAGGGGCUACC	5'		21
				.|.o|||||||||||o|||			
HvEOL1			5'	AAUUCCAGGGCUCCCCGGUGG	3'		
Fg-sRNA-6717	86	4.5	3'	UAGCUUGGGUCCCGAGGGGCUAC	5'		23
				||..|.o||||||||||o||			
HvEOL1			5'	AUGAAUUCCAGGGCUCCCCGGUG	3'		
Fg-sRNA-1921	416	6	3'	CUUGGGUCCCGAGGGGCUACC	5'		21
				|.||.|||||.||.|||||||			
HvSERK2			5'	GCACGCAGGGGUCACCGAUGG	3'		
Fg-sRNA-321	2106	4.5	3'	GCUUGGGUCCCGAGGGGCUACC	5'		22
				o|.||.||||||||||.||||			
HvBAK1			5'	UGCACACAGGGCUCCCCCAUGG	3'		
Fg-sRNA-1921	416	4	3'	CUUGGGUCCCGAGGGGCUACC	5'		21
				|.||.||||||||||.||||			
HvBAK1			5'	GCACACAGGGCUCCCCCAUGG	3'		
Fg-sRNA-6717	86	5.5	3'	UAGCUUGGGUCCCGAGGGGCUAC	5'		23
				.|o|.||.||||||||||.|||			
HvBAK1			5'	UUUGCACACAGGGCUCCCCCAUG	3'		
Fg-sRNA-321	2106	5.5	3'	GCUUGGGUCCCGAGGGGCUACC	5'		22
				..|.o|||||||||o|||o|||			
BdEOL1			5'	GAAUUCCAGGGCUCUCCGGUGG	3'		
Fg-sRNA-1921	416	4.5	3'	CUUGGGUCCCGAGGGGCUACC	5'		21
				.|.o|||||||||o|||o|||			
BdEOL1			5'	AAUUCCAGGGCUCUCCGGUGG	3'		
Fg-sRNA-6717	86	5.5	3'	UAGCUUGGGUCCCGAGGGGCUAC	5'		23
				||..|.o|||||||||o|||o||			
BEOL1			5'	AUGAAUUCCAGGGCUCUCCGGUG	3'		
Fg-sRNA-321	2106	3.5	3'	GCUUGGGUCCCGAGGGGCUACC	5'		22
				o|.||.||.||||||||||||			
BdSERK2			5'	UGCACGCAAGGCUCCCCGAUGG	3'		
Fg-sRNA-1921	416	3	3'	CUUGGGUCCCGAGGGGCUACC	5'		21
				|.||.||.||||||||||||			
BdSERK2			5'	GCACGCAAGGCUCCCCGAUGG	3'		
Fg-sRNA-6717	86	5.5	3'	UAGCUUGGGUCCCGAGGGGCUAC	5'		23
				..o|.||.||.||||||||||			
BdSERK2			5'	UCUGCACGCAAGGCUCCCCGAUG	3'		

904 Mismatches (MMs) between mRNA and sRNA are marked as ".", while G-U pairs are marked

905 as "o".

906

907

Figure legends

Fig. 1: Virulence of Fusarium graminearum strains PH1 and IFA65 DCL single and dKO mutants on barley and Brachypodium.

A: Relative infected area on leaves of barley cv. Golden Promise (GP) at 5 dpi. Detached leaves were inoculated with 3 µl of a solution containing 150,000 conidia per mL. The area with leaf necrosis was measured with the free image analysis software package PlantCV. Boxplots represent the median and quartiles of three independent biological experiments (n=56). (Wilcoxon Rank Sum Test, $P=7.1*10^{-3}$, x=mean)

B: Relative infected leaf area on leaves of *Brachypodium distachyon* Bd21-3 at 5 dpi. Detached leaves were inoculated with 10 µl of a solution containing 10,000 conidia per mL. The area with leaf necrosis was measured with ImageJ. Boxplots represent the median and quartiles of nine independent biological experiments (n=63). (Pairwise Wilcoxon Rank Sum Test, Bonferroni corrected, $P_{dcl1}=4.9*10^{-8}$, $P_{dcl2}=2.6*10^{-4}$, x=mean)

Outliers (>2.5) are not shown but indicated as written values next to the upward arrow (↑).

Fig. 2: Relative expression (log2 fold) of potential barley target genes for fungal sRNAs in leaves infected with Fusarium graminearum wt strain PH1 vs. PH1-dcl1/2.

Expression was normalized against barley *Ubiquitin* (*HvUBQ*) and subsequently against the Δct of the uninfected control (mock treatment). Bars represent the mean±SE of three independent biological replicates. Significant differences were calculated for the expression of a respective gene in PH1 vs. PH1-*dcl1/2*-infected samples and PH1 vs. controls. The dotted line shows the expression level of mock treatment. (Student‘s *t*-test, (paired) one sided, *P<0.1, **P<0.05, ***P<0.01)

Fig. 3: Relative expression of HvEOL1 in response to inoculation of barley leaves with Fusarium graminearum.

A, Relative expression of *FgDCL1* and *FgDCL2* on detached barley cv. Golden Promise leaves at 5 dpi in wt strain IFA65 and 7 days post spray application of the 1,782 nt long dsRNA construct dsRNA-*dcl1/2* vs. TE buffer. **B**, Relative expression of *HvEOL1* at 5 dpi with IFA65 vs. mock control. **C**, Relative expression of *HvEOL1* 5 dpi with wt strain IFA65 and 7 days post spray application of dsRNA-*dcl1/2* vs. TE buffer. Gene expression was first normalized against the reference gene *HvUBQ (HORVU1Hr1G023660)* and subsequently against the Δct of the respective control for B (mock = 0.002% Tween20) and for A,C (IFA65 / TE). Bars represent the mean ± SE of three (B) and four (A, C) independent biological replicates. (Student‘s *t*-test, *P<0.05, ***P<0,005)

Fig. 4: Relative amount of different fungal tRFs with homology to HvEOL1 mRNA

Relative amount of different fungal tRFs with homology to *HvEOL1* mRNA during infection of barley leaves with PH1 and PH1-*dcl1/2* normalized to fungal biomass and relative quantity of sRNAs normalized to wt PH1 measured by qPCR. *Fg*-sRNA-1921, *Fg*-sRNA-321 and *Fg*-sRNA-6717 quantity was normalized to *Hvu*-miR159 and *Hvu*-miR168 and fungal biomass as determined by *FgEF1α* expression was normalized to *HvUBQ*. Subsequently the amount of sRNAs was normalized with fungal biomass. The amount of sRNA in PH1-infected leaves was set to 1. Values and error bars represent the mean ± SE of three independent biological replicates. Significance was calculated via a one-sample *t*-test. (**P<0.01, ***P<0.005)

Fig. 5: Relative expression of BdSERK2 in response to inoculation of Brachypodium distachyon leaves with Fusarium graminearum.

956 Relative expression of *BdSERK2* in detached Bd21-3 leaves at 4 dpi with PH1 vs. PH1-*dcl1/2*.
957 The gene expression was first normalized against the reference gene *BdUBI4* and subsequently
958 against the Δct of the mock treated control. Values and error bars represent the mean ± SE of
959 three independent biological replicates. (Student‘s t-test, paired, one sided, **P<0,01)

960

961 ***Fig. 6: Analysis of potential target sites of Fg-sRNAs as determined by RLM-RACE products.***

962 **A,B,C** Potential target sites of *Fg*-sRNA-321 and *Fg*-sRNA-1921 predicted by TAPIR (blue),
963 genomic DNA (GPv1, GCA_902500625.1, A: contig7:321364603-321365033, B:
964 contig2:598018255-598018555, C: contig2:474465508-474465708) of barley cv. Golden
965 Promise (green), and the alignment of sequences derived from the RLM-RACE PCR (red)
966 relative to the *Hv*-gDNA and *Fg*-sRNAs. **D,E,F** PCR-products of the second nested RLM-
967 RACE-PCR visualized in an EtBr-Agarose gel. Red arrows indicate excised bands and blue
968 arrows indicate infection specific products.

969

970 ***Fig. 7: The degree of DCL-dependent gene silencing is correlated with the number of***
971 ***homologous fungal sRNAs.***

972 Each dot represents a predicted target gene of *Fg*-sRNAs. On the x-axis the ΔΔΔct-value is
973 shown with bars representing SD. On the y-axis the $\log_2$ of the number of total sRNAs
974 potentially targeting each gene are shown. The dotted line represents a linear regression model.
975 P indicates the significance (t-test) of the model and the score cut-off indicates the score limit
976 used during the target prediction. Plot A, B, C and D are the calculations for a score cut off of
977 3, 4, 5 and 6 respectively.

978

979

980 ***Tab. S1: Primer sequences***

Gene	Accession	Primer Name	Sequence
HvARF3	HORVU1Hr1G076690	HORVU1Hr1G076690_F	GGTTCAGCTCAGAAACGAAGC
		HORVU1Hr1G076690_R	ATTCTGACGCTCCACTCCTTG
HvPPR	HORVU2Hr1G078260	HORVU2Hr1G078260_F	GGGTGCTTCATCGAGTTGGAA
		HORVU2Hr1G078260_R	CTGCAAAACCACAGAGCTTGT
HvSERK2	HORVU2Hr1G080020	HORVU2Hr1G080020.6_F	GATGACAGACAGAGTCCTGCT
		HORVU2Hr1G080020.6_R	AGCACTACTACCAGCACCGA
HvARF10	HORVU2Hr1G089670	HORVU2Hr1G089670_F	CACATCGGCGATGAACCTTTC
		HORVU2Hr1G089670_R	TCGGCTCAAGATCGATGGATG
HvPGLP2	HORVU5Hr1G052320	HORVU5Hr1G052320_F	CTCCTTGTTCTGTCAGGTGTGA
		HORVU5Hr1G052320_R	ATTGCTGGTGCTGTATTCGGA
HvATG2	HORVU6Hr1G034660	HORVU6Hr1G034660_F	TTCTTATCTCGGGGCTTGGTG
		HORVU6Hr1G034660_R	TCGTAGCAGCCAAGAACCATT
HvGDH	HORVU6Hr1G076880	HORVU6Hr1G076880_F	GGCAACGTGGAGAGTGTGAA
		HORVU6Hr1G076880_R	GTACGGGCTCGAGTTGATCAG
HvARF19	HORVU7Hr1G096460	HORVU7Hr1G096460_F	GGGCCGGTCTATCGACATTAG
		HORVU7Hr1G096460_R	TTGACAAACTCCTCCCAAGGG
HvSUB1	HORVU2Hr1G028070	MLOC_12796.1_F	CAGAGTTCAGGAGGGGCAAG
		MLOC_12796.1_R	GACAAACGTCCGGTTGAGGA
HvSUVR5	HORVU6Hr1G069350	MLOC_14605.1_F	TGCATTTTGTTGACCGCAGG
		MLOC_14605.1_R	AGGCTTGTCTGGGAACGATG
Hvemb2726	HORVU5Hr1G024470	MLOC_58105.1_F	AGACTGATGTTGCGGTGGAG
		MLOC_58105.1_R	GGTTGCGACCTAACTTGGGA
HvPIX7	HORVU3Hr1G051080	MLOC_5991.1_F	GATGGGCTTCAGGGGCATAA
		MLOC_5991.1_R	ATGGGAGCGGAAATGACCTC
HvRDR1	HORVU6Hr1G074180	MLOC_75294.1_F	TATCTGAAGGTTCGGCCTGC
		MLOC_75294.1_R	GTTCCGCTCCACAGAACAGA

HvRST1	HORVU3Hr1G016630	MLOC_75306.1_F	TTGCGGGACTTGTTCTTGGT
		MLOC_75306.1_R	TGACAGATGGCAGAGCAAGG
HvEOL1	HORVU2Hr1G119180	MLOC_8741_F	CACTTCAAGCCCGCTGACTA
		MLOC_8741_R	CTCATGTATCGTGCTCGCCT
BdSERK2	BRADI_5g12227v3	PNT61220_F	AGTTGCGTTTCCTCCGTCTT
		PNT61220_R	ACCAGTTGATGGAACCTCTCC
HvUBI	HORVU1Hr1G023660	Ubideg60_F	ACCCTCGCCGACTACAACAT
		Ubideg60_R	CAGTAGTGGCGGTCGAAGTG
FgEF1a	FGSG_08811	EF1a_F	CAAGGCCGTCGAGAAGTCCAC
		EF1a_R	TGCCAACATGATCATTTCGTCGTA

Name	**Sequence (RNA)**	**Primer**	**Sequence (Primer)**
***Hvu*-miRNA-159a**	UUUGGAUUGAAGGGAGCUCUG	hvu-mir159a_F	TGGCTCGCTtttggattgaaggga
		hvu-mir159a_RT	GTCGTATCCAGTGCAGGGTCCGAGGTATTCGCACTGGATACGACcagagc
***Hvu*-miRNA-168**	UCGCUUGGUGCAGAUCGGGAC	hvu-mir168-5p_F	GTTCGCTtcgcttggtgcagat
		hvu-mir168-5p_RT	GTCGTATCCAGTGCAGGGTCCGAGGTATTCGCACTGGATACGACgtcccg
***Fg*-sRNA-321**	GCUUGGGUCCCGAGGGGCUACC	Fg-sRNA_321-2106_F	TCGCTccatcggggagccctg
		Fg-sRNA_321-2106_RT	GTCGTATCCAGTGCAGGGTCCGAGGTATTCGCACTGGATACGACcgaacc
***Fg*-sRNA-1921**	CUUGGGUCCCGAGGGGCUACC	Fg-sRNA_1921-416_F	TCGCTccatcggggagccct

		Fg-sRNA_1921-416_RT	GTCGTATCCAGTGCAGGGTCCGA GGTATTCGCACTGGATACGACgaacc c
***Fg*-sRNA-6717**	UAGCUUGGGUCCCGAGGGGCUA C	Fg-sRNA_6717-86_F	TCGCTcatcggggagccctggg
		Fg-sRNA_6717-86_RT	GTCGTATCCAGTGCAGGGTCCGA GGTATTCGCACTGGATACGACatcga a
Universal SL Reverse		UniSL_R	CCAGTGCAGGGTCCGAGGTA

Target	**Accession**	**Name**	**Sequence**
RLM-adapter		RLM_Adapter	GCUGAUGGCGAUGAAUGAACACU G CGUUUGCUGGCUUUGAUGAAA
RLM outer adapter Primer		RLM_Uni_O1	GCTGATGGCGATGAATGAACACTG
RLM inner adapter primer		RLM_Uni_I1	GAACACTGCGTTTGCTGGCTTTGAT G
HvEOL1	HORVU2Hr1G119180	HvEOL1_outer	GAATTTACTGATGGCCCGCAT
	HORVU2Hr1G119180	HvEOL1_inner	ACCCACCATTAAGCATCGCA
HvSERK2	HORVU2Hr1G080020	HvSERK2_1_outer	GAGCCTCAGGAGACGGTTTT
	HORVU2Hr1G080020	HvSERK2_1_inner	AGTGGAGTCGACGATCCAGT
HvBAK1	HORVU7Hr1G068990	HvSERK2_2_outer	GGGTTTGCACATGCTCGTAC
	HORVU7Hr1G068990	HvSERK2_2_inner	TGAGGACCCAGCTCTACCTC

981

982

Fig. 1

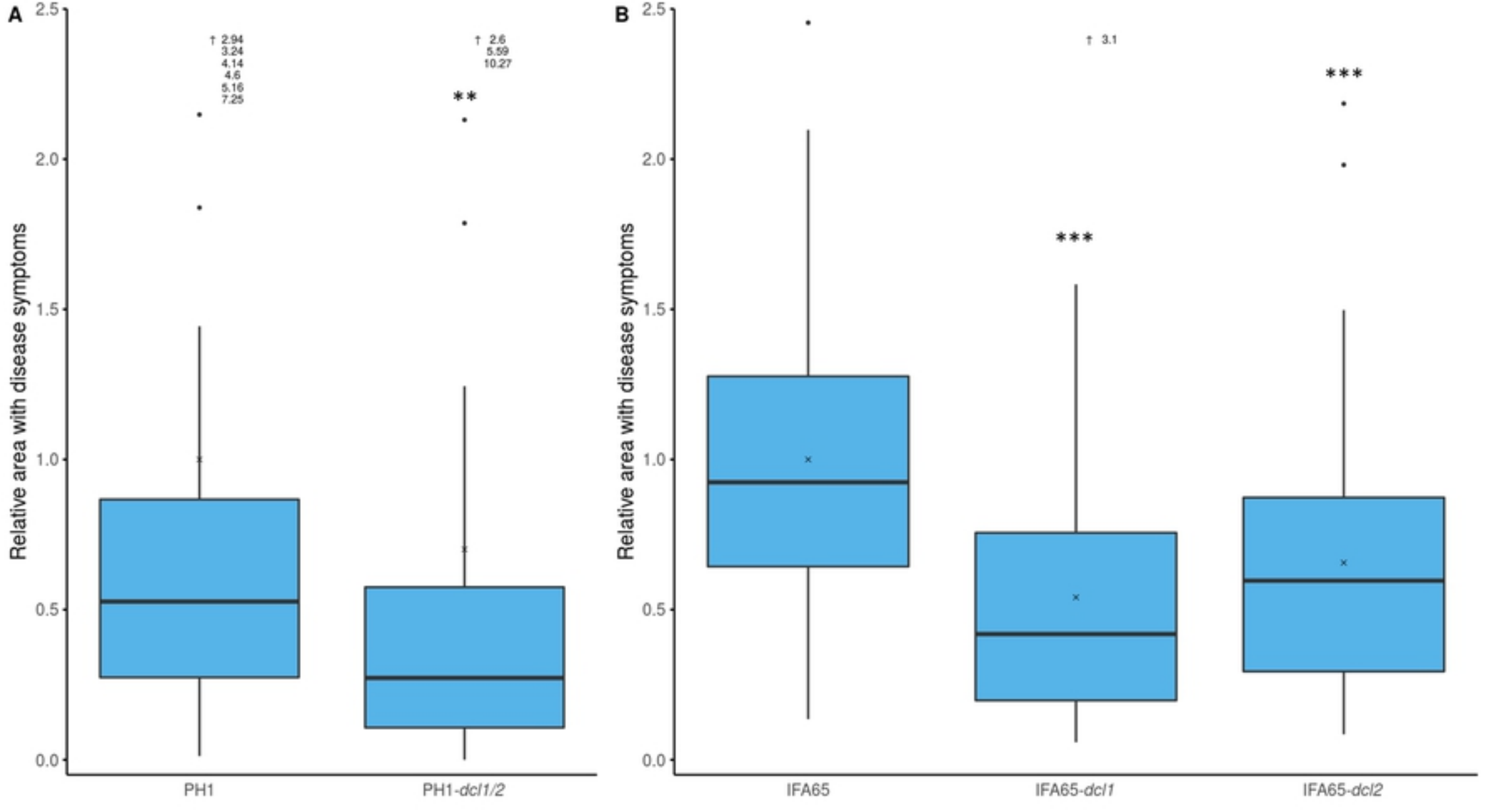

Figure 1

Fig. 2

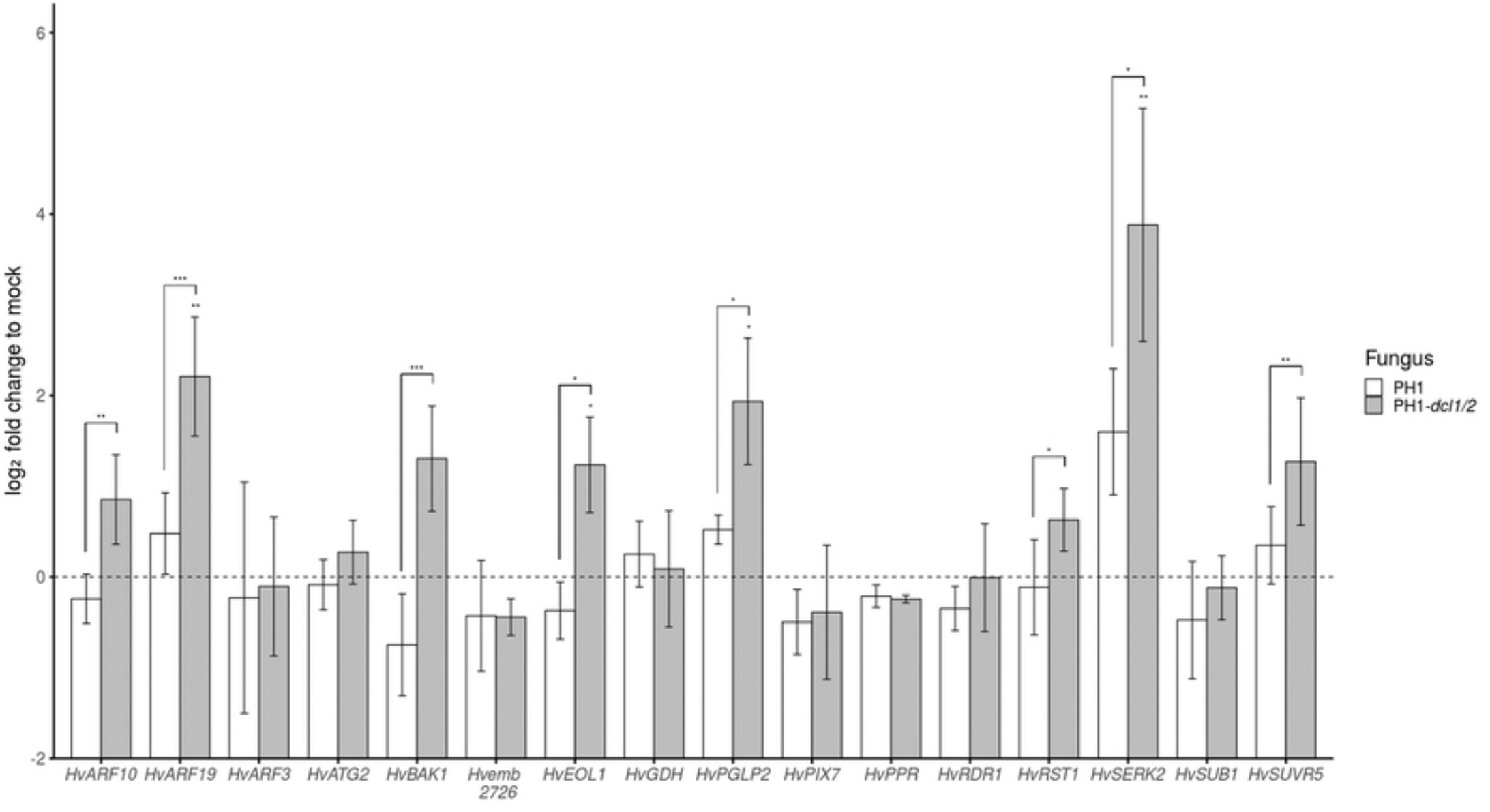

Figure 2

Fig. 3

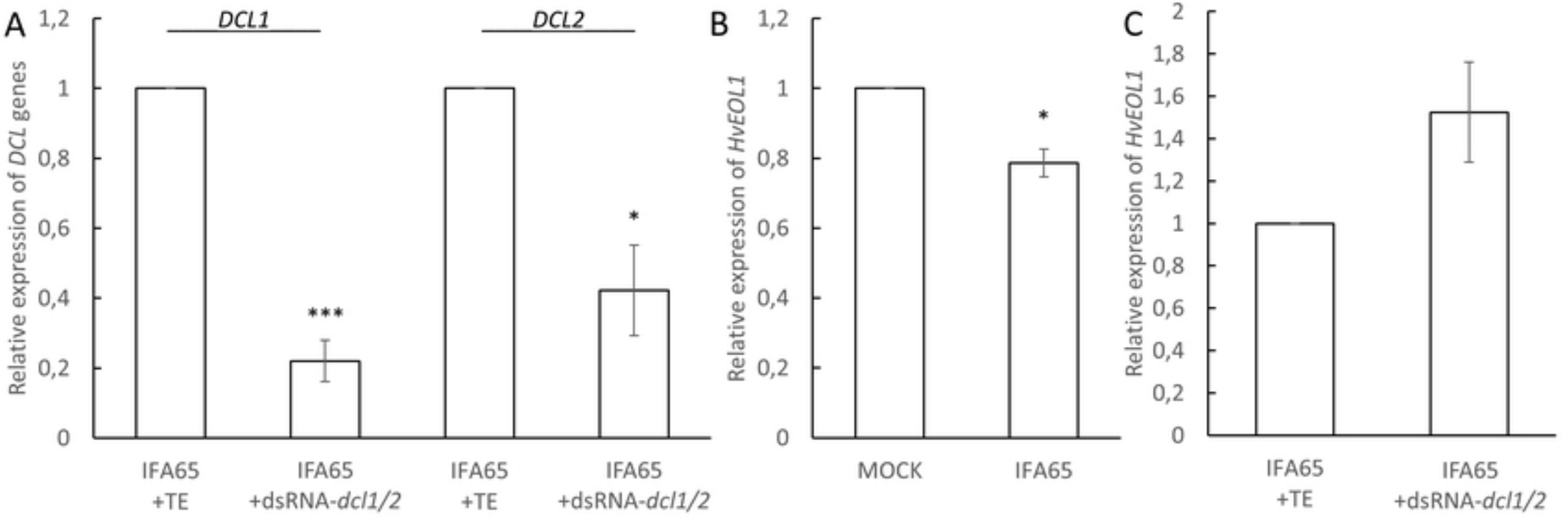

Figure 3

Fig. 4

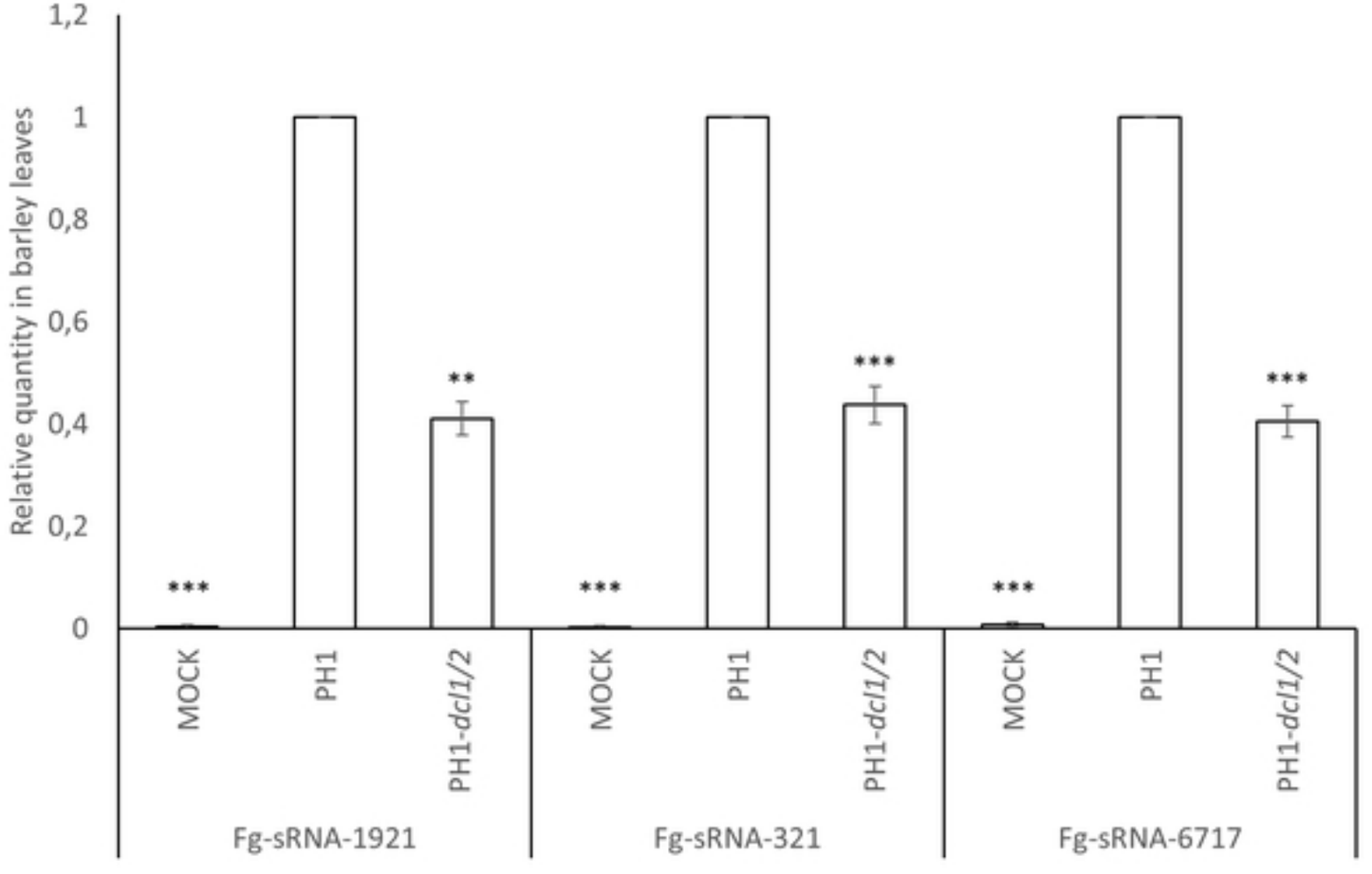

Figure 4

Fig. 5

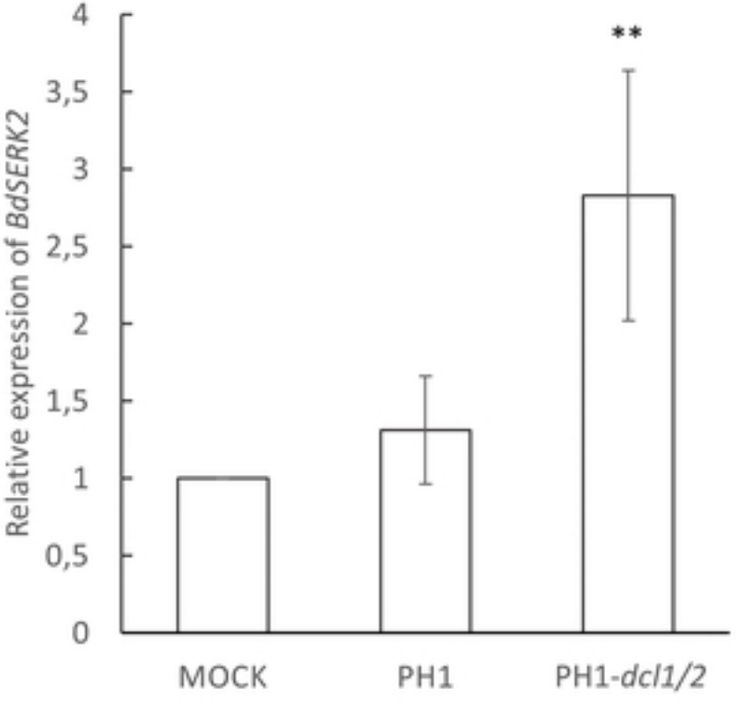

Figure 5

Fig. 6

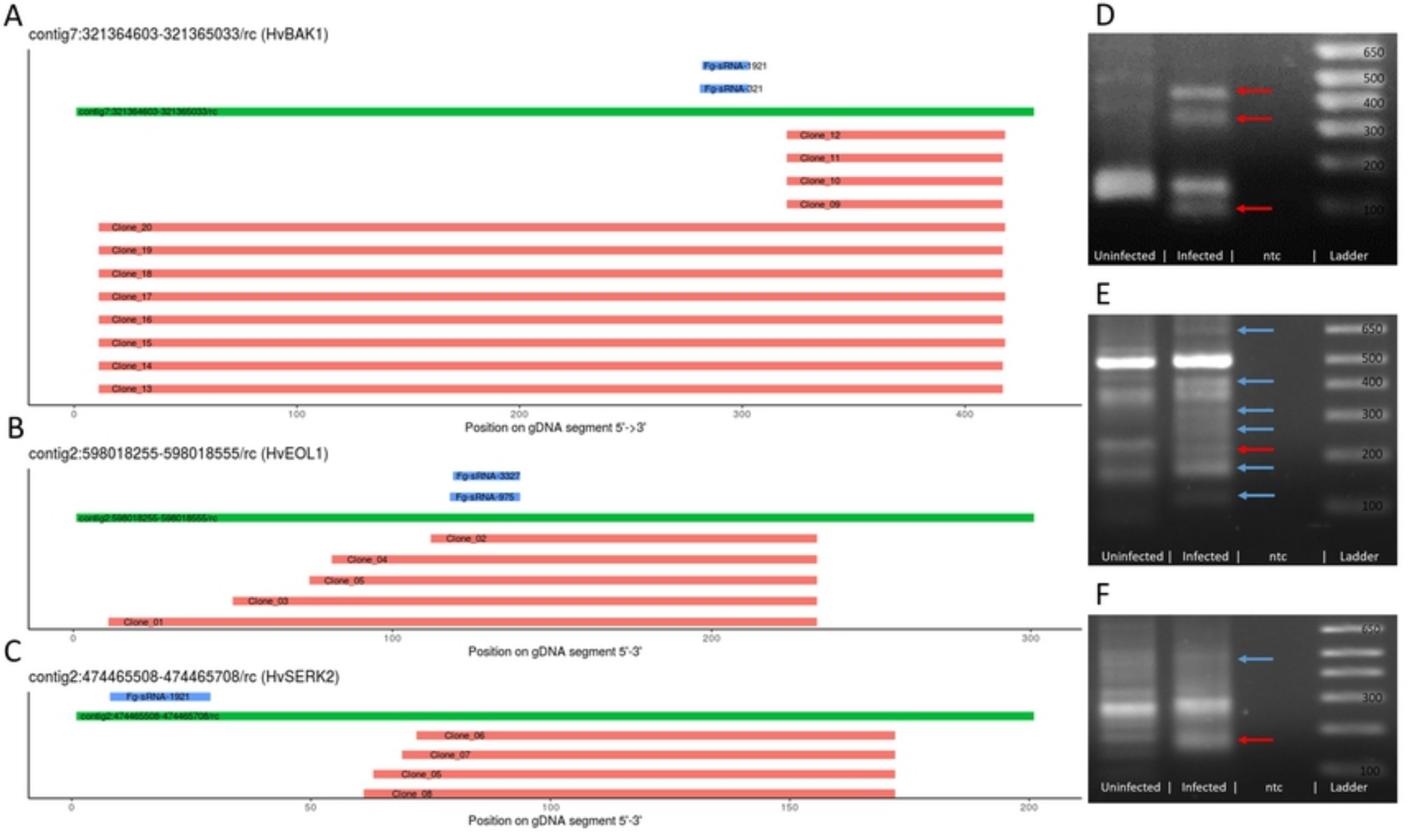

Figure 6

Fig. 7

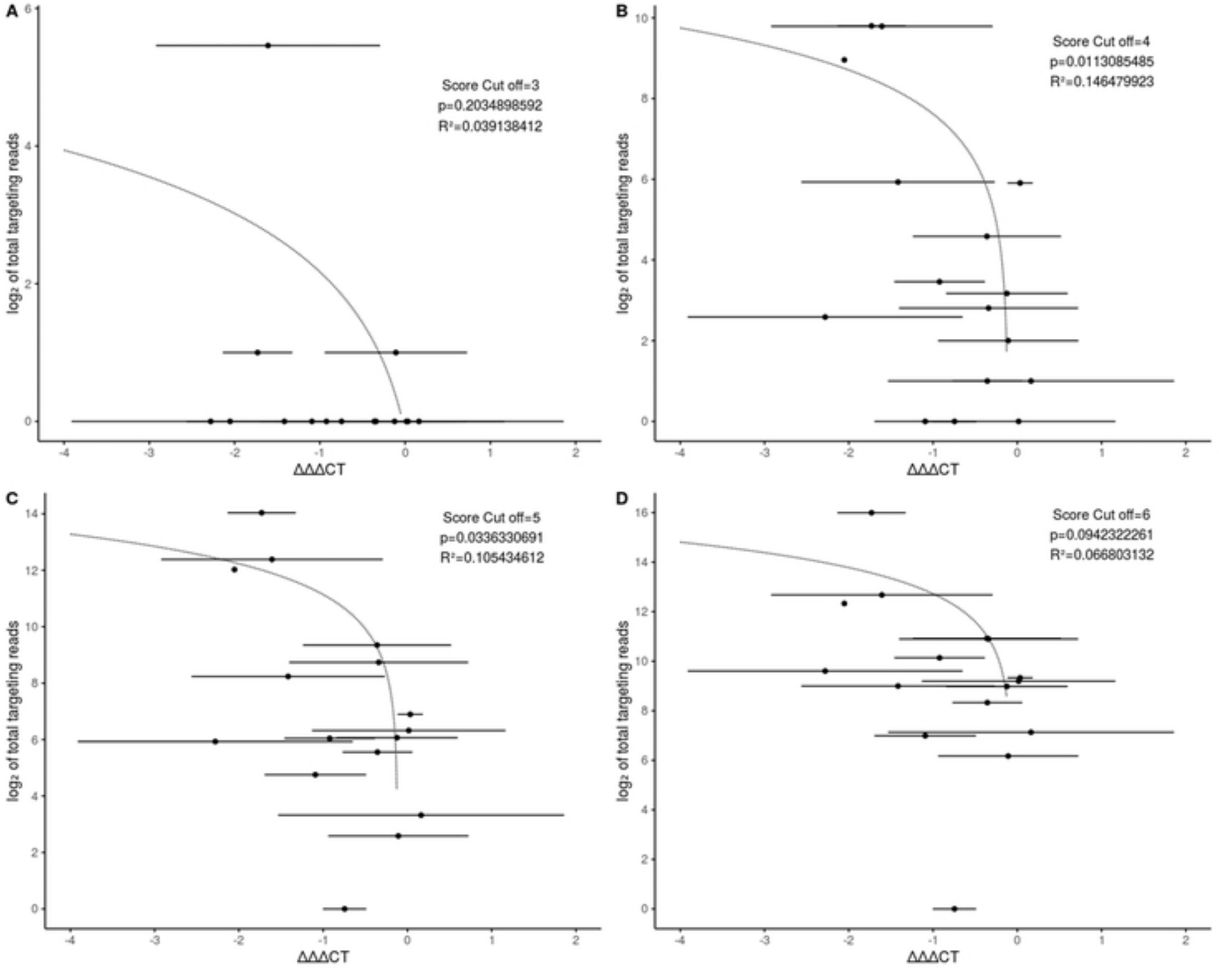

Figure 7

Fig. S1

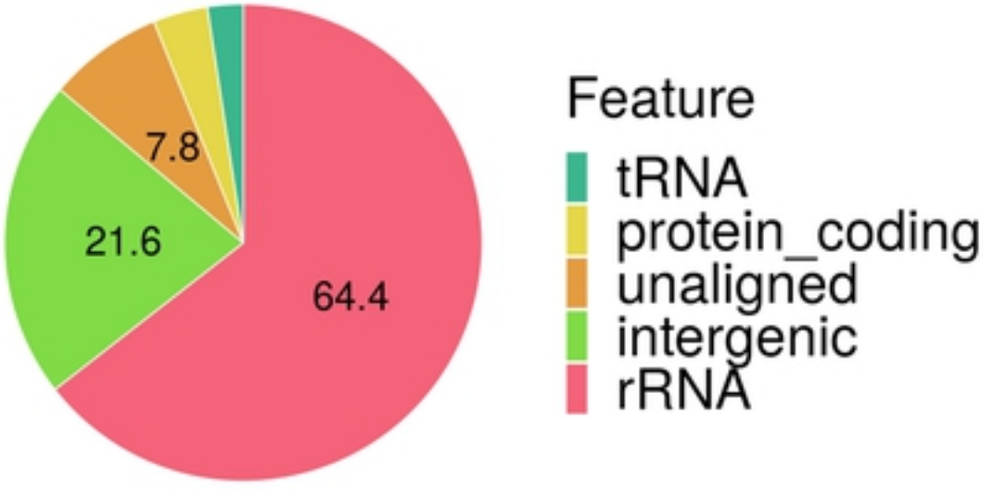

Feature	Counts	%
rRNA	3517854	64.4
intergenic	1181441	21.6
unaligned	423796	7.8
protein_coding	204681	3.7
tRNA	132329	2.4

Figure S1

Fig. S2

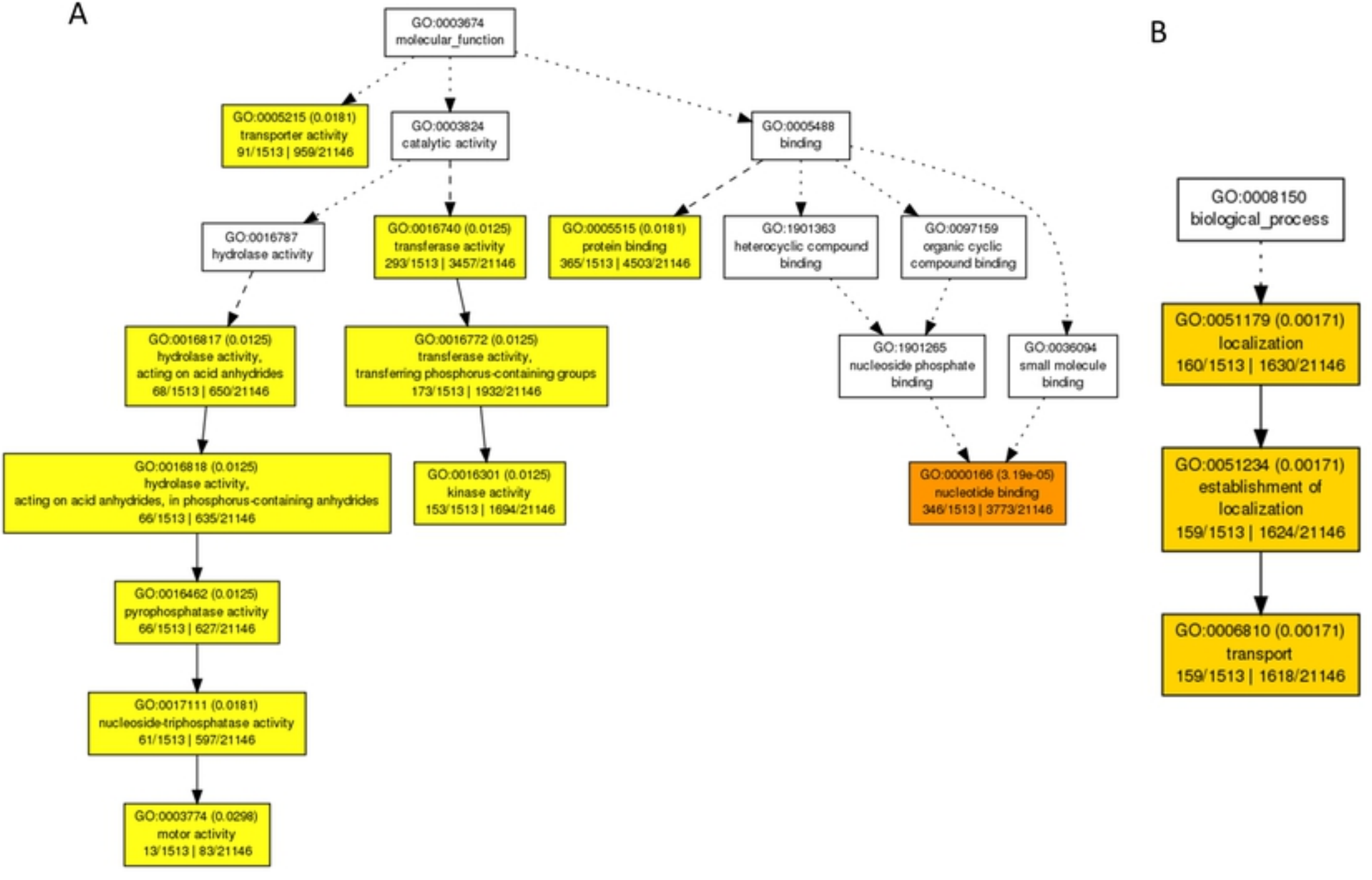

Figure S2

Fig. S3

Figure S3

Fig. S4

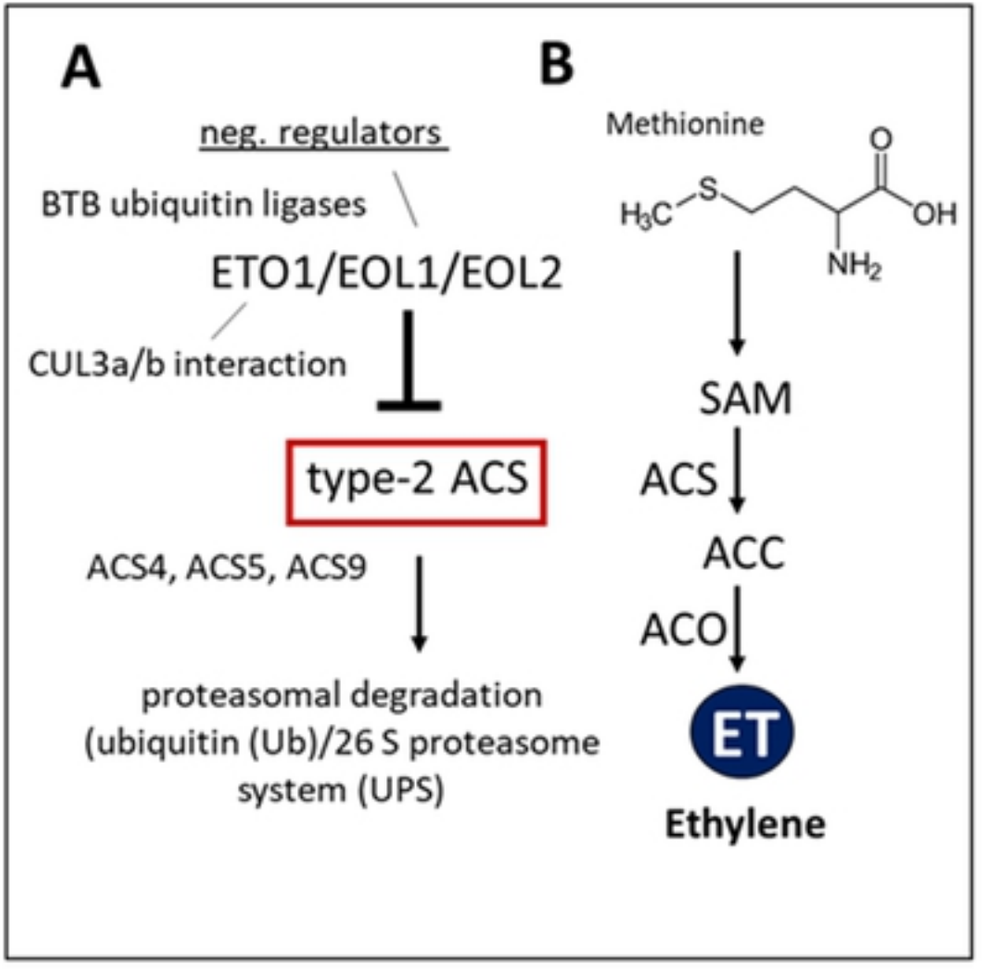

Figure S4

Fig. S5A

FgDCL1-FGSG_09025

ATGGACACCGACTCGACCGACAGCGAAGATGATCGCGTTCAGTATCGCCTGACCGTGAGGCCTTCGAAGCATCGAAAGAATACAGAGAAGAAGCGCCTGAACAAGCAGGTTTTGAAA
CAATACATGATAGAACACGACAGAGAAGCCTATGCCAAAGATTCTGAGAAAAAGAAGCGCGGCCCCTTCGCTGAAGCTTCCACCGACATTACACCGCGAGAATATCAGATAGAACTCT
TCGAAGCCGCCAAGGAGAAGAATCTCATTGTGGTTTTACCTACAGGTATTTTCTTGTCCCTTTCTGACTCTACTCTGGACATTCTAATAGGCACAGGTTCTGGTAAAACACTCATCTCCAT
CTTATTGCTAAAATACTACATTCGAATCGAAGTGGAATCTCGCGCTCTTGGAAATCCGAGGAAGGTGGCCTTTTTCTTGGTGGAAAAAGTAGCCCTCTGTGAGCAGCAATACCGATTTC
TTAAGGACCAGATTTTCGGCCACAACATTGTCATGTTCACAGGCGATAACCGCGGCGTGACCAAGGACAAGAAGTACTGGGATGATCAGTTTTCCTCAAACAAGGTTGTGGTCTGCAC
TGCTCACATTTTGCTCGACTGTCTGAACAACGGCTTCATTACAATGGACCAGATCAACCTCCTCATCTTCGACGAAGCCCATCATGCAAAGAAGAAGCATGATTACGCGCAAATTGTCC
GACGATATTATTATTCTACCGAAAAGAACAAGAGACCTCGCATTCTAGGAATGACCGCTTCCCCTGTGGATTCCAAGGCTGGAGATGTTGCAGAACTGGCACTTGAACTTGAGAAAAC
CCTTGACAGCGAGATCGCAACACTCTCCGACAAGATGATGCGACAGGCGACTGATTTCCAAGTTCATGTTGAAGAGACAGTCAAATACAACACACTTGGACTACCAGACGAGACCAAG
ACACAGCTTTGGGACTCGATCTCTAAGCTAGTATCGCGAAACAAGGAATTCAAGGCGTCTCTCGACTTCACAAAAGAGGCCTCCACAATCCTAGGACCCTGGTGTGCGGACCGATACT
GGCAAGTCTTGATCGACGATACAGAGATCAAGCGACTCGCCGACAGGACTCGCATGGCTTTTTTCGGGGGTGGAGAGAAGTTGTTGGCAAGAGGAGACCAAGCAGAAGAGGCTGTC
AGGGAGGTTCAAAAGGTCGTCGCAGCCCACGAGTTTAGGGCGATCAGTCCTCAATCGCAGGAATTGTCAGCTAAAGTGAAATGTCTACATGAAATCCTGGTTCATGCCTTCACAGTCG
ATAACACAAAGCGCTGCATCGTTTTTGTTGATCAGAGACACACAGCTTGCCTCCTTTCGGACCTTTACGACCAAGTTTCAATGGCAATTCCCGGTATGAATGCTTCGTATATGGTAAGTT
GAGTCCCATTTCCAACAGCAGTAACTAACCACAATAGATTGGTCAACAATCTAGCAGCAGCACCCTTGGCAATATGTCTCTGCGAAAGCAATGTTCAACGCTCAAGAACTTTAGGGACG
GCGTGATAAACTGTCTCTTTGCAACATCAGTGGCAGAGGAGGGAATTGACATTCCGAGTTGTGATCTTGTTATCCGATTTGATCTCTATACTTCTGTTATTCAGTATGTTCAATCCAAAG
GGCGTGCGAGACACGAATCTTCACGGTATATCACCATGCTGGAAGACGGCAACATGAGACAGATTCGCAGTCTGAAACAAGCAGCGAGAGATGCAACAGCCCTTCGAGAGTTCTGTC
TAAGAATACCTGCCGATCGAAAACTTCAAGACGATGTATTTGATGAGGAGACGGAAAGTCAGATCAAGCAAATACGTTTTAACGTGTACAAAATAGAATCAACGGGCGCACAACTTAC
ATTCCCCTCAAGCCTCGAGATACTAGCTCGATTCGTTGCATCCTTGGGTACAGCAGAGAGCAGCCATAGCAAGGCTGAATATCACGTCTACAAGGTGGGAACATATTTCACAGCCGCC
GTCAATCTACCGTCCAGTTCCCCCATCGTCTCCCAAACAGGCTATCCACAACGAAGCAAGCTTCTCGCAAAATGCTCAGCGGCTTTTGAGGTTTGCAAGAAGCTCATCAATGGCAAACA
CATTGATGATCATCTTCAGCCTACTTTCAAGAAACATTTCCACAAAATGCGCAATGCTCGTGTGGGAATAAGCCCTAACAAGAAGGGTGAGCATGACATGCGCCTGAGGCCCAACGTTT
GGAGTATCCGTGGAGAATGGACACACTTCTTCCCAACAAGAATTACTCTTGACAGGGATTGTGGAGAGAAAAACAGGTCGTTGATTCTTCTTTCGCGAAGTCCACTTCCAGGACTACCT
TCAATCCCTCTATTCTTCGGCAATGGACGCTCAGCCATCGTTGAAGTGACATGTTCTCAAGAACCTTTACCCATCACGACCGAGGAAGCTGGGGGTTTGACTGCTTTCACACTCAAAATC
TTTGCCGACGTTTTCAGTAAAGAGTTTGAGGCCACTTGCGACCAGTTTCCTTACCTTCTTGCCCCCTTGGCAAAAGACACCAATCTAAACGAAATATCGCGAATCGACTGGGATACTGTC
AACCTTGTCAGAGACCATGACAGTCTCGAATGGGAGAATGCGCCCGACGATTTCTTTTTCGACAAGCTTGTTGTAGATCCATATGATGGAGGGCGCAAGCTTATAATCAAAGGCATTG
ACAAATCCAAGAAGCCTTCTGATCCTACACCGGAGGGAGTGCCTGAGTCGAGAAGTCGTGCTTATAGGTCTGCGGAACAAAACATTAAGCAGTACAGCAACAGTCTGTTTTCCAAGTC
TCGACTAACGGCCCAGTGGCGAGACGATCAACCGGTTGTCAAAGCTGAGCTTCTCTCATTGCGACGCAATCTGTTGGACGAGTTTCAAGTAAACGAGGAAATCAACAAGGATTGCTTC
GTCATTTTAGAACCCCTCAACGTGTCACCTGTAAGTGAAAGACTCTTCTGTAAAACGTATCTAACATGCCCAGCTGCCAATTGACGTCGTTTCCATGGCACTCAAGTTCCCGGCAATCAT
CCACAGAATCGATTCTGCTCTGATCGCTCTTGATGCATGCGAACTATTCGACCTCTCTATTCCGCCAGCGCTGGCACTCGAGGCAATGACCAAAGACAGCGACAACACTGAGGATCATG
GCAAGCAACAAATCAATTTCCAAGCTGGCATGGGTTCCAACTATGAAAGGTTGGAATTTCTTGGAGACTCGTTTCTCAAAATGGCCACCACAATCTCCATTTTTGTACTCAAACCCAAGA
GCAACGAATGTTTGTACCATGTAGAGCGCATGCTGCTCATCTGCAACAACAATCTGTTCAACACGGCCGTAGATTGCAAGCTCCCAGAGTACATACGATCCTTGGCATTCGACAGGCG
AACTTGGTACCCTGATCTTACACTCAGAAAAGGCAAAGCTTTCAAGGCAACAGCGCGACAGCGCTTAGCCGACAAAAGTATTGCGGATGTCTGTGAAGCTCTCATTGGTGCTGCATAC
CTCTCAAGCAAGGATGACAATTTGAACATGGCCGTCAAAGCTGTGTCACAGATGTGCAAAGCAAAGTACCATACCATGATGGCTTACGATGAGTACTACGCATCTTTCAAGGTTCCAG
ATTGGCAGAAAGCCAGTCCAAACGCCAACCAGCGTAGACTTGTGCAGAAAGTGGCAGACGCTACCGGGTACCACTTCAAGTCTGCGCCGCTGCTCCAGAGTGCATTCACACACCCTTC
TTACGCGTATTCAGGGAACGTTCCAAACTATCAACGCCTCGAGTTTCTAGGCGATGCCCTCATCGACATGACCATCGTCGAATATCTCTATCGCAACTTTCCCCTCGCAGACCCTCAGTG
GTTGACGGAGCACAAGATGGCAATGGCCTCGAACCAATTTCTCGGTTGTCTGTGTGTTAAGCTCAATCTGCACCACCATCTTCTGTTCAACACGTCGCAGTTCATCAGCAAAATTCGTG
ACTATGTGGCCGAACTTGAGTTGGCTGAAGAGACTGCGCGCCAAGAGGCAGAAGAAGACGGGACTCCAATGCGCATGGACTTTTGGCTCAATGCGACAACGCCTCCAAAAGCGTACG
CAGATTCAATCGAGGCTCTTATGGGGGCCATGTTTGTGGATTCTGAATTCGACTATTCTGTTGTTGAGGATTTCTTTACCAAGTTCATCTTCCCGTACTTTAAAGACATGTCTCTGTACGA
TACCTTTGCAAACAAGCATCCTTACACATTTCTCACCAAGAAGATGCAACAGGAGATCGGGTGCATGAAATTCTGTATGATTTCAGACACCCGCGTTCCTGATGCAGAGCGTGGCATGG
AAGTTATGAAAGAGTACGACATATATTCAGCCTTTCAAGTGCACGAAAGAGTCATCACATGTCACGTATCAAAGAGTGGAAGGTACGGTAAGATTGCTGCTGCAAAGGGGGCACTCG
AGTTGTTGGAGCCGTATGGCGGTGATGTGGTCGCGATGAAGAAGCTGTTGGGCTGCGACTGCGACTCTGTAACAGCAGCCATGGCGGAGATGGACCATGGAACAGCTGTCTAA

Figure S5A

Fig. S5B

FgDCL2-FGSG_04408

ATGTCCTCAAGCGATAAGGTCATGGCGGACGCCTCTTCCATACCAGACTCCGAGGTCAAAACAATAGCGTCGTCCTCGGTCGTCGAGATCTCTGCTACAGGCGAGAAGGAGATAACGA
CTCATATACCTGTCGCAGATACACCAATGTGCTCAGATGACCAGGCCAATGTGCAAGAGCAAGACGAAGAAGTTAAGCCTCAGAAAGTGACGCCCAATCCAGAGGTGGTAAATCCCC
GCGGTTACCAGCGAGAGATGCTGGAACAAAGCATCAAAAGGAATGTCATCGTTGCAGTAAGTTATTCCAAGTACCCCATTCAATCTGCATTCGGTGACCTGATTAGATGGACACGGGA
AGTGGTAAAACTCAAGTGTATGTCACTTCCATACCATCGAAAAAGAGAGAGACTAATTATAACTCGTAGGGCCGTGATGCGCATCCAACATGAACTCGATACATGTGCACCAGACAAG
GTTGGTGAACAAAGAAACATAATATCGCGGTCAAAACTAACCAATATAGATTATCTGGTTCTTAGGCAAGACAGTATCGCTATGTGAACAGCAATACAGCGTTGTCCAAAGGCAAATG
CCGTCGGTATCGATGAAACTGCTAACGGGGCAATTGAACATCGATGCATGGTCCGAGGACGTCTGGCCCCGTATCCTTAATGGGACTCGTATCATTGTCTCGACCTTTGATATCCTGCG
AGATGCTTTGGACCATGCATTTGTCAAGATGAACATGCTGTCCCTTATCGTCTTCGATGAAGGTGAGACATCGCCAACACTTACAATATCATTACTGACTTTTTACAGTTCATAATTGTGT
AAAGAATAGCTCTGGTCGAAAGGTTATGGTGAATTTCTATCACGAACACAAGAACGCCGGCATGCCCGTGCCTGCTATCCTGGGTTTAACAGCCAGCCCGATACAGTCGAAGTCAATC
CACGACGAAATCCTTGAGCTCGAGGTCACCATGGATGCTGTATGCATCACTCCAACAATTAACCGGAAAGAACTCCTCCAGCACGTCAACAAGCCCAATCTTTCCCGAGTATTGTATGA
TGTGGAAGAGCATCCGACTCGAACCCCCCTAATGCAGACTCTGCAGTCTGAGTACTCGGCGATGGACATCACCCAGGACCCAAGTATTATAAAGGCCAAGCAACTTATCGCTAAGGGC
GAGAAGACTGGACCTGAAATACTAAGTATGTTGATGAAACACAGGACCTTCTCTCAGAAGCAGTTAAAGTCCTTATGGAACAAAAGCAAAGACATTCTTGATGAACTCGGGCCTTGGG
CTGCTGACAAGTACATCTCCGAGTTGGTCAGTCTGTTTCTCAAGAGAATCGACTCGCCAATGACGTTTAACGAGTCCTGGAGCAATGAGGATAGGACCTACCTCGCAGGTCATTTGAG
ACAGATCGCTGCCAGTCCCCATCAGCCCAAACTACCAGACAGACACAACTTGGCCGACAAGACGAATAAACTAATCCAGGAACTACTTGCAGCGGATGAAGATGTGGTCGGCATTATA
TTCGTCAGATCAAGGGCTGCTGCCAACGTCCTTTGTGCTCTTTTGAGGGAGCACCCCGAGATTCGACAGCGATATCGAGTCGGCTCTGTAGTAGGATCCGCAGCCACCAAGATTCGAA
AGCAAAACATCTACGAGTATCTGCCCGGCGCGACTGCCGATACATTACGCGATTTCAAAACAGGCGCCATCAACCTTTTGGTCTCGACTAGTGTTCTTGAAGAGGGTATTGATGTCGCA
GTGTGCAACCTCGTCATATGTTTCGATGAGACAACGACACTCAAGTCCCATATCCAACGCCGCGGACGAGCTCGCAAACAAAAATCAAAGATGATAGTACTTGCTAGATCTTCATCCGA
CGCTCGGGAATGGGATTCCCTAGAAAGAGACATGAAGAGTCGTTATGAGCAGGAAAGGGGAGAGTTGGACGCTTTAGAGATAGAGGCTCGCACTGAAGCGACGTCCTCTTTTTCTTA
TACTGTGAAAAACTCAGGGGCTAGATTGGACCTCGAGAATTCTCGCCAGCATCTGGAACATTTTTGTAACAAGGTTTTCCAGCGAGATTACGTTGATCCGAGACCCGTCTACATTTTCC
ACAAGACCGAACTGGGATCAGCACCGCCGACTTTCAGCGCAACGGTGACTCTTCCCTCGGGTCTGCCTAAGCACCTCCGAAGGTGCCAAGGTGGAGGTGGATGGAGATCAGAAAAGA
ATGCGATGAAGGAAGCGGCTTTTCGTGCATTCGTCATGCTGCACCAAGAAGGTTTGGTTAGCGACCACCTTCTTCCCCTAAATGCAGATTCGAAAGAAGCAGAAGAAGAGGTGCAGCT
AACTGCGCCCGAGCTTCTATTTGACCCATGGAAAGACATTGCACAGCGGTGGGAGACCACGGCTGAGAAATGGCTCTATGCTTACGAGTTCGCCGATCACGAGTATGTTACTCCTCTTC
ATTTCGAGATTGCCTTGCCTGTGTGTCTTCCACGACCCCGCGACATCACCTTTCATCCTGAAGAGGGACTTAAATGGCATGTCAAATGCACCTCAATCAAGAGGATCTCCAATGATGAAT
GCTTGGGCTTGCCAGATCATACGTCAACCCTATTGGCGATGCATTATGGCCACCGCTGGAACGTGGAAGATCGTGACCATGTGATCAAATTCATATATGAGAACAAGAATCTCACCCG
AGATCAAATTGGATCGGTACCCTTCGGCGAAAGCATTGATGCTCTATTGGAAAAGAGAGTCCTGGTTCGGGACCCCAAAAATACTCCCTTCCACTACGTCAAAATGATCCCATCAAAGC
CTCCAAAAGAGCAAGTTCAGCACCCATTTAATGAATACGAGGAAGCGCCAGAAGAACAGTATCTAGTTGTGGATCAATGGACACGCAGGTCGGACCTGTTGCATGAGATAAAACCCG
GTCAGGGGAAGAGCTCTTGCACCAAACCCTACCGCTGGGTTCTCCCGATTTCCAGAGCGACTGTTGATGAGGTTCCTCGGCGTGCCGCTAAGTGCGGTATGCTTATCCCTTCCATCATT
CACGAATTGGAGGTTCAGCTCATCGCGAATGAACTGTCCTCGACACTTTTGGCGCCAGTTGGTATCACAGATCTGCAATTGGTGATTGAAGCCATCAGCTCGCGTAGCGCTGCAGAGC
CTGTTGACTATGAACGTATTGAATTTTTGGGCGATTCGGTTTTGAAGTATTGCACTGTTATTCAAGCCTACTCTGAACGTAAGTCTTCCGCATCCCTCTATCGTCACTTTCACTGATCATT
GTCACAGATCCCTTTTGGCCCGAAGGTCTACTCAACCATTTCAAAGACCGACTAGTCTCCAATACCCGTTTGACTCGCATGTGCCTTGAGACAGGCCTTTCCAAGTTCATTTTTTCCAAAA
CATTTACTGGAATCAAGTGGAGACCGCTATATCGAGACGAATTCCTAGATAAGAAGCCAGTCGATGGTGTATCAAGGTTTGTTGGTCCAAAGACTCTTGCTGATGTGGTCGAGGCACT
TGTTGGAGCCTCCTACCAGGATGGAGGAATCAGCAAAGCTCTGGAGTGCATCAAGGTTTTCTTGGGCACCAAGTGCAATTGGCATGATGACAAAGTCGCCAGAGACATACTCTTCCGA
GCAGCAATTAGCGACGTACCGTTGCCCCCCACGATGGAGCCTTTGGAAGAGCTCATCGGGTACACATTTCAGAAGAAGTCTCTACTCATTGAGGCAATGACTCACGGGTCGTATGCGG
CTGATGGGCAGCAGCGATCTTATGAACAACTCGAGTTTCTTGGAGATGCGGTTCTTGACTACATTGTCGTAACCCGAATGTTCCAATCTGACCCCCCAGTGCCCAATGGACGCTTACAC
ATGGTCAAGACTGCCATGGCCAACGCTGATTTCCTTGCTTTTACAAACATGCAACATGGACTACGCCGGCCTGAAGTTGAAATAAATGAGAACGGCGAACCAGTGCCTACAGAAGTTT
CACTGCCGATATGGAAATTCATGCGTCATAGCTCTCCAGAGATGGGTAGAATCATGAATGAGACCCAGGCCCGATTTGAGAGCCTTCAAGAGGAAATCAATGAGGCTAGGACGAATG
GTAAACACTACCCCTGGACACTTCTCGCTCGTCTTCACCCGAAGAAGTTCTACTCCGATATTTTCGAGGCTACCCTAGGTGCCATTTGGGTTGATTCAGGAGATATCGAAGTATGCACA
GCCTTTCTTCACAAGTTCGGCGTCTTGCCGTATCTTGACCGAATTCTCAGCGATAATATTCATGTTCAACATCCTAAAGAGGAACTCGCCAAACTAGCAATCGACCAGAAAATGACGTAT
GATTATACGGCTGTTGATGGGCCTATAAAGGAGTACCTCTGCACGGCCAAGGTTGGAGATCGCGTCGTGGGAGTCGTGTCAGGGGCACTCAATAAGGCTGAGGCAATGACCAAGGCT
GCCGAAGAGGGCGTGAATTTTTTGAATGGGGAGCAGAAACGTGCAGAGAAGGCGGCTCAGGATGAAATGGCGCGATTTCTTGTTGCCATGGAACTCATTTAG

Figure S5B

Fig. S6

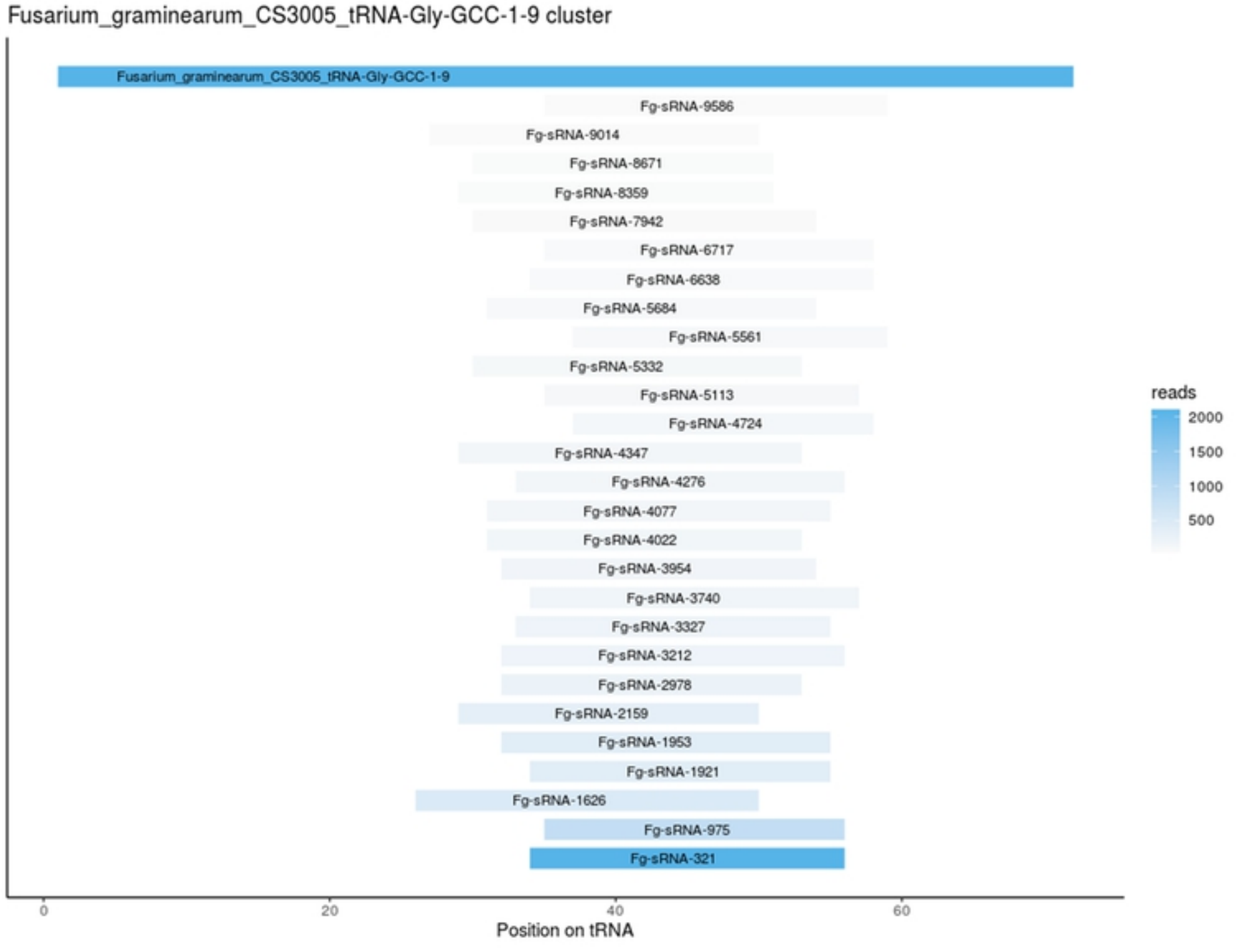

Figure S6

Fig. S7:

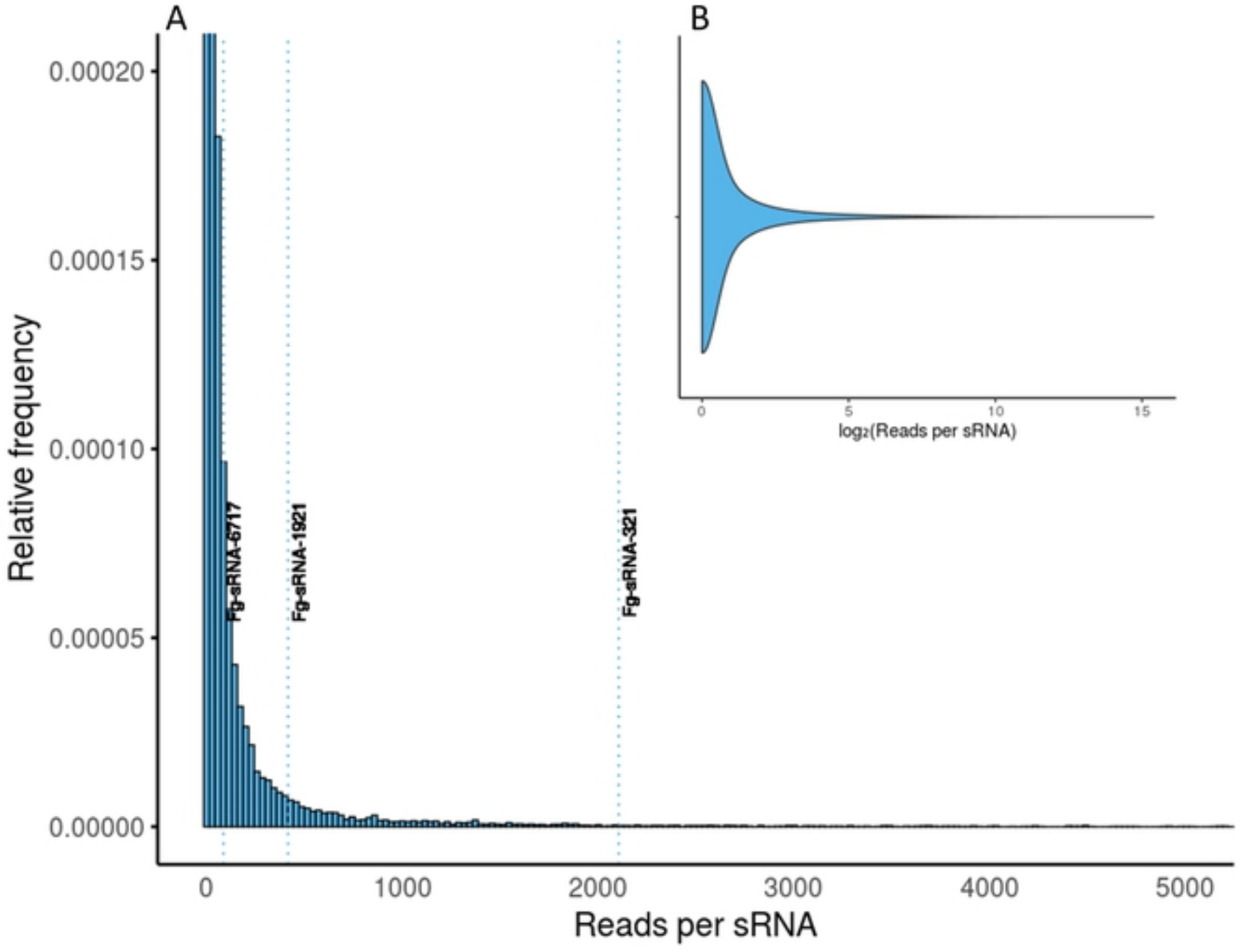
A
B
0.00020
0.00015
0.00010
0.00005
0.00000
Relative frequency
Fg-sRNA-6717
Fg-sRNA-1921
Fg-sRNA-321
0
1000
2000
3000
4000
5000
Reads per sRNA
0
5
10
15
log2(Reads per sRNA)

Fig. S8

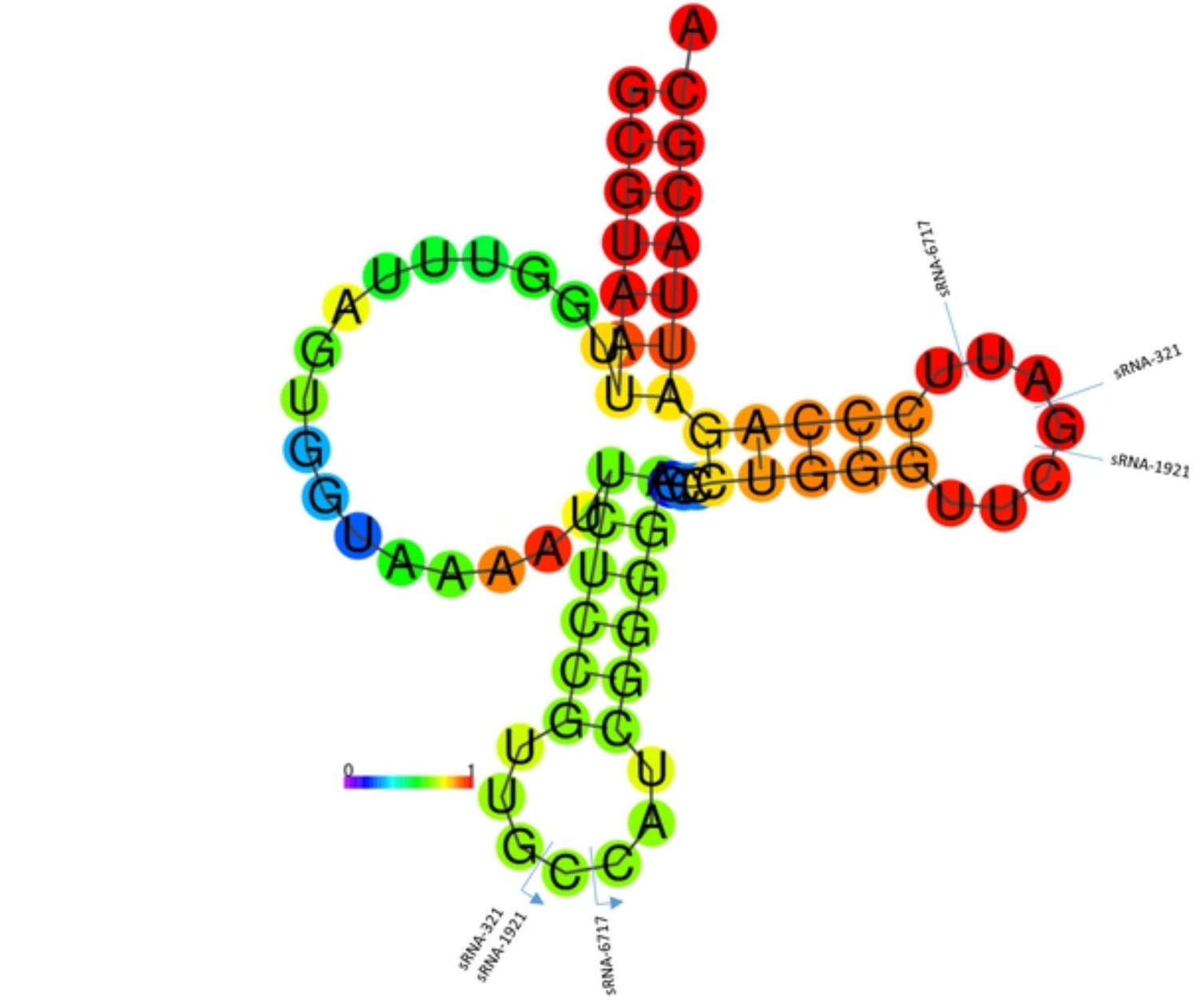


```
>Fg-sRNA-321                                                                                    CCAUCGGGGAGCCCUGGGUUCG
>Fg-sRNA-1921                                                                                   CCAUCGGGGAGCCCUGGGUUC
>Fg-sRNA-6717                                                                                    CAUCGGGGAGCCCUGGGUUCGAU
>lcl|Query_57046 Fusarium_graminearum_CS3005_tRNA-Gly-GCC-1-9 GCGUAAUUGGUUUAGUGGUAAAAUUCUCCGUUGCCAUCGGGGAGCCCUGGGUUCGAUUCCCAGAUUACGCA
 centroid secondary structure                                 (((((((.................((((((.......))))))...(((((.......)))))))))))).
```

Figure S8

Fig. S9

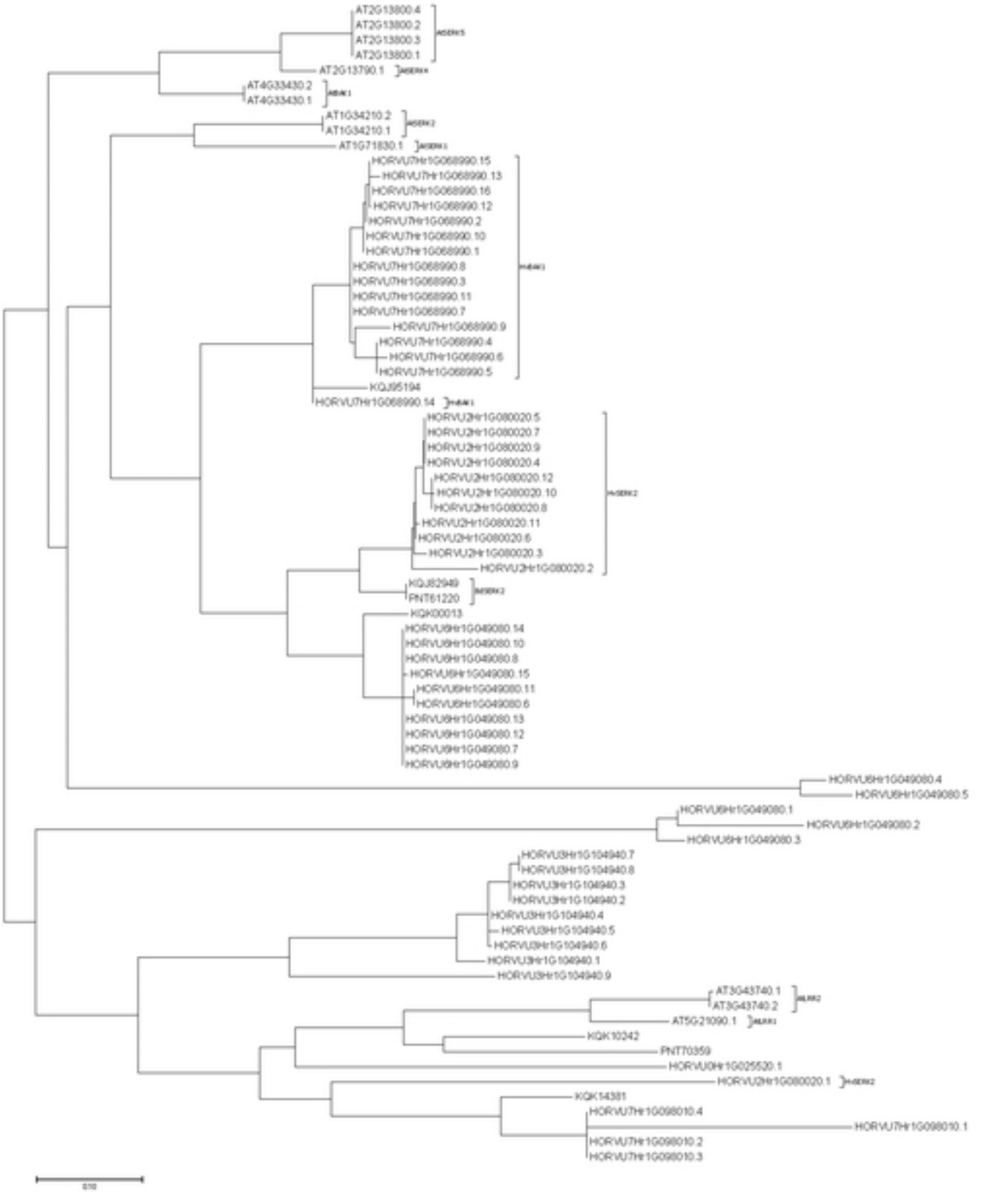

Figure S9